Desirability-based optimization of dual-fuel diesel engine using acetylene as an alternative fuel

Van Giao Nguyen [a], Brijesh Dager [b], Ajay Chhillar [b], Prabhakar Sharma [b, **],
Sameh M. Osman [c], Duc Trong Nguyen Le [d, ***], Jerzy Kowalski [e], Thanh Hai Truong [f],
Prem Shanker Yadav [g, h], Dao Nam Cao [f], Viet Dung Tran [f, *]

[a] *Institute of Engineering, HUTECH University, Ho Chi Minh City, Viet Nam*
[b] *Department of Mechanical Engineering, Delhi Skill and Entrepreneurship University, Delhi, 110089, India*
[c] *Chemistry Department, College of Science, King Saud University, P.O. Box 2455, Riyadh, 11451, Saudi Arabia*
[d] *Faculty of Automotive Engineering, Dong A University, Danang, Viet Nam*
[e] *Departament of Mechanical Engineering and Ship Technology, Institute of Naval Architecture, Gdańsk University of Technology, Gdańsk, Poland*
[f] *PATET Research Group, Ho Chi Minh City University of Transport, Ho Chi Minh City, Viet Nam*
[g] *Department of Mechanical Engineering, JSS Academy of Technical Education, Noida, India*
[h] *Centre for Advance Studies in Vehicle Diagnostic in Research in Automobile Engineering, Delhi Technological University, Delhi, India*

HIGHLIGHTS

- Engine performance and emissions fuelled with acetylene/diesel were analyzed.
- The box-Behnken design was employed for the Design of Experiments.
- 4.48 lpm AGFR, 27.1 % BTE, and 76.58 bar Pmax are the optimized results.
- Tweedie has a better R^2 and MSE performance than LightGBM.

ARTICLE INFO

ABSTRACT

The study examined the dual-fuel engine performance employing acetylene gas as primary fuel and diesel as pilot fuel. The engine's operational parameters were adjusted using the Box-Behnken design, and the results were recorded. The best operating settings were yielded as 81.25 % engine load, 4.48 lpm acetylene gas flow rate and the compression ratio were 18. At this optimized setting the BTE was 27.1 % and the engine emitted 360 ppm of NOx, 56.2 ppm of HC, 104 ppm of CO. The experimental data at optimized setting was compared to the optimized results, and the percentage of errors was within 7 %. Two advanced machine learning methods, LightGBM and Tweedie, were used to predict engine efficiency and emissions. Tweedie-based models had an R2 value of 0.89–1, while LightGBM-based models had an R2 value of 0.38–1. The mean squared error was 0.24–45.04 for Tweedie-based models and 8.5 to 153.89 for LightGBM-based models. On the basis of R2 and MSE, it was observed that Tweedie was superior at making predictions than LightGBM. The study demonstrated the efficient functioning of a dual-fuel engine using acetylene as an alternative fuel for increased performance and lower emissions.

---

* PATET Research Group, Ho Chi Minh City University of Transport, Ho Chi Minh City, Viet Nam
** Department of Mechanical Engineering, Delhi Skill and Entrepreneurship University, Delhi, 110089, India
*** Faculty of Automotive Engineering, Dong A University, Danang, Viet Nam
E-mail addresses: psharmahal@gmail.com (P. Sharma), nguyenldt@donga.edu.vn (D.T. Nguyen Le), dungtv@ut.edu.vn (V.D. Tran).

List of nomenclature

AGFR	Acetylene Gas Flow Rate
ANN	Artificial Neural Networks
BDC	Bottom Dead Centre
BTE	Brake Thermal Efficiency
CCD	Central Composite Design
CO	Carbon Monoxide
CO_2	Carbon Dioxide
CR	Compression Ratio
C_2H_2	Acetylene
DoE	Design of Experiment
DF	Dual-fuel
ER	Equivalence ratio
GFR	Gas flow rate
GHG	Greenhouse Gases
ICEs	Internal Combustion Engines
H_2	Hydrogen
HC	Hydrocarbon
LCV	Lower Calorific Value
LightGBM	Light Gradient Boosting Machine
LPM	Liters per Minute
m	Mass
MSE	Mean Squared Error
ML	Machine Learning
MAPE	Mean Absolute Percentage Error
MAE	Mean Absolute Error
MBT	Minimum Spark Timing for Best Torque
NOx	Oxides of Nitrogen
P	Pressure
Pmax	Peak Cylinder Pressure
R^2	Coefficient of determinations
RE	Relative Error
RSM	Response Surface Methodology
SI	Spark Ignition
T	Temperature
TDC	Top Dead Centre
LHV	Lower heating value
UHC	Unburnt Hydrocarbons
USD	United States Dollars

1. Introduction

Nowadays, humans are abusing natural resources at an alarmingly high pace to make their lives more pleasant and comfortable [1,2], in which humans are constructing heavy industries to obtain a high level of comfort, which has resulted in a multiplication of energy requirements in recent years [3,4]. In addition, rapid urbanization and industrialization along with the fast-growing human population are resulting in shortage of energy sources and environmental pollution [5–7]. Due to this reason, massive deforestation and thorough exploitation of natural sources are necessary to meet enormous energy demand [8,9], which raises serious concerns about global warming, declining natural assets that are limited in nature, energy security, and environmental concerns [10,11]. In addition, massive deforestation along with the use of fossil fuels for energy and power production are found to increase CO_2 and greenhouse gas emissions [12,13], resulting in a serious climate change in the world. Facing the depletion of fossil fuels and climate change, society has begun to consider eco-friendly development which needs high technological advancements relating to alternative fuel and renewable energy sources to slow down this consumption of fossils especially in the transportation sector as there is leap and bound progress in the number of vehicles [14–16]. As a result, finding alternate fuels and renewable energy is critical to compensate the ever-increasing shortage of energy and reduce the climate change, as well as target sustainable development goals of nations and areas [17–19].

Indeed, with the continuous depletion of fossil fuels and environmental damage, experts all over the world are looking for viable replacement fuels [20,21] aiming to satisfy two main goals of diversification of provided fuels and reduction of pollutant emissions [22,23]. As reported in the literature, there have been many type of potential alternative fuels such as biodiesel [24,25], biogas/syn-

gas [26,27], bio-oil from pyrolysis [28], alcohol (methanol, ethanol, propanol, butanol) [29–31], furan [32,33], ether [34,35], hydrogen [36,37], natural gas [38,39], and others. As it can be created using non-fossil sources like calcium carbide and water, acetylene (C_2H_2) has been proposed as a potential replacement for fossil source-based fuels [40,41]. Acetylene generation depends on the process used, the price of the raw materials, the price of the energy, and other aspects. As of 2023, it's estimated using data from the local market that using calcium carbide to react with water will generate acetylene at a cheap price of about 0.4–0.5 USD per cubic meter. Contrary to what has been observed, acetylene is highly explosive, so flashback arrestor use is always advisable as a safety measure. Acetylene has properties such as being a colorless gas with a distinct garlic-like odour, being highly flammable, having an ignition temperature around 305 °C, having a high flame speed, etc. Due to all these distinct physical and chemical characteristics, acetylene is an intriguing prospective fuel for internal combustion engines (ICEs) [42,43].

Acetylene is one such fuel that can be used in ICEs because acetylene has a rapid speed of flame as well as low ignition energy, which can result in enhanced combustion efficiency and lower pollution emissions [44,45]. Acetylene has the potential to be a fuel for high-performance engines, including motorcycle, and racing vehicle engines, due to its high calorific value and fast flame [46,47]. Acetylene as a fuel for transportation is still in the trial stage, and no nation has widely adopted it because of its low energy density [48]. It is also quite challenging to store and transport acetylene because this gas is prone to breaking down at higher temperatures and pressures, and hence it is considered a highly unstable gas, which reduces its economic viability as a fuel for transportation [49]. Acetone-soaked porous materials like diatomaceous earth or activated charcoal are used to fill the cylinders used to store and transport acetylene. The acetone dissolves the acetylene and prevents it from breaking down, which aids in stabilizing it [50].

Acetylene as an alternative fuel for ICEs has been the subject of several experimental research in the past. ilhak et al. [51] experimentally carried out a performance and exhaust emission analysis of four-stroke water-cooled SI engine fuel using a mixture of gasoline and acetylene at various loads and flow rates of acetylene. It has been noted that with the induction of acetylene, not only does the overall thermal efficiency reduce, but there is also a significant drop in hydrocarbon emissions at all loads and a modest rise in NO at low loads. To reduce NOx, Hilden et al. [52] studied the engine performance and exhaust emission behavior of an SI engine with acetylene as the fuel. This study team maintained consistent engine speed, constant airflow, and MBT spark timing throughout the studies. Equivalence ratios between 0.43 and 0.53 and compression ratios between 4 and 6 are ideal because preignition began at compression ratios higher than 6. Although acetylene fuelling results in a decrease in power and thermal efficiency when compared to petrol fuel, it also generates little pollutants. In addition, ilhak et al. [53] advocated that ethanol and acetylene would be good substitutes for petrol as they can be easily derived from renewable sources and thus evaluated this fuel along with petrol for exhaust emission and performance of a multi-cylinder, four-stroke, water-cooled Ford SI engine at different load settings at a constant speed. They found that NOx formation and UHC emissions were reduced to a very large extent with this ethanol and acetylene. Because this acetylene has a low octane number of 50, it is susceptible to knocking, which can be overcome by supplying a lean mixture. Choudhary et al. [54] tested the engine for the performance of a diesel-acetylene fuel combination on a single-cylinder water-cooled four-stroke CI engine with a variable compression ratio. It has been reported that engines operate better at greater compression ratios of 19.5:1, although emission characteristics are better at lower compression ratios of 18:1. Sharma et al. [55] conducted an extensive study in India to identify the optimal flow rate of acetylene between 50 and 200 LPM that best suited the engine characteristics of SI engines driven by a combination of petrol and acetylene. The results mimic that at a flow rate of 100 LPM acetylene provides very little emission and hence using this optimum fuel flow rate various engine performances and exhaust emission characterization have been carried out. It has also been discovered that small anomalous acetylene combustion occurs exclusively at greater loads. The research findings of this research group stated that acetylene has a strong ability to replace petrol in the near future. Gupta et al. [42] turned a four-stroke SI engine into a six-stroke engine by injecting water at the end of the recompression stroke to assess and compare the performance of petrol and acetylene as fuels independently. When utilized in a six-stroke engine, acetylene exhibited encouraging results when compared to petrol, with a 45 % increase in thermal efficiency and a considerable reduction in exhaust emissions when compared to a four-stroke engine. The results of the exhaustive experimental examination showed that combining acetylene with the modified six-stroke engine increased engine performance and emissions. In light of its combustion properties, Lakshmanan et al. [56] investigated acetylene gas as fuel in air-cooled single-cylinder direct injection CI engines under variable load scenarios as an alternative to diesel fuel in dual fuel mode. In this case, diesel was employed as the primary fuel and acetylene as the supplementary fuel. The engine performance worsened with this dual fuel, and there was a reduction in smoke, CO, and UHC owing to improved combustion, as well as an increase in NOx production and peak pressure due to high-speed flame propagation.

Acetylene-diesel dual fuel compression ignition (CI) engines are being investigated as a potential alternative to standard diesel engines. Despite substantial research in this area, some crucial research gaps must be filled to increase our understanding and optimization of these engines. To begin, there are no comprehensive studies that investigate the combined effects of engine load, CR, and acetylene gas flow rate (AGFR) on the performance, combustion characteristics, and emissions of acetylene-diesel dual fuel CI engines in the existing literature. Most studies have focused on single factors, with little systematic investigation of the interaction between several control variables and their overall impact on engine performance. Also, while RSM has been demonstrated to be an effective optimization tool for a variety of engine systems, its application to acetylene-diesel dual fuel CI engines remains limited. The full potential of RSM in this context must be investigated and leveraged to determine the optimal operating conditions for these engines in terms of efficacy, emissions, and overall performance [57]. The major goal of this study work is to fill the gaps described above by performing a thorough examination of the effects of engine load, CR, and AGFR on the performance of acetylene-diesel dual fuel CI engines. It will be achieved by using RSM as a strong optimization tool to determine the ideal operating parameters that result in the best trade-off between engine efficiency, emissions reduction, and overall efficiency. This study also intends to give useful insights into the combustion properties and pollutant production mechanisms in acetylene-diesel dual fuel CI engines, particularly under diverse operating situations. The findings of this study will help to improve our understanding of the underlying mechanisms and will

aid in the design and development of improved and environmentally friendly dual-fuel CI engines. A schematic of the research in this study is depicted in Fig. 1.

2. Materials and methods

2.1. Test setup

In the present investigation, the experiments were carried out on a research engine with a maximum load capacity of 3.5 kW. As shown in Fig. 2, the test engine is naturally aspirated and capable of accepting variations in operating characteristics such as injection timings and loading conditions. The engine was a single-cylinder and four-stroke, and it has provision for loading using an eddy current dynamometer. The engine had provisions for varying the compression ratio. The major specifications of the test engine are described in the authors' prior work. The fuel injection system consists of an injector with three circular holes of 0.3 mm diameter spraying diesel at a 120° angle, a fuel pump made by Bosh, and a fuel filter. In this study, the fuel injection pressure was maintained at 220 bar.

The baseline test was started by operating the engine in diesel mode. Initially, the test engine was run at a lower operating setting i.e., CR = 167.5 and FIT = 23°bTDC) for five different levels of engine loadings (20 %, 40 %, 60 %, 80 %, and 100 %). The engine is operated with high-speed diesel as pilot fuel. The acetylene gas was drawn from an industrial-grade gas cylinder using a digital gas regulator. It was ensured that fire extinguishers were available nearby to test setup and proper ventilation was ensured. In addition, the main properties of the test fuel are listed in Table 1.

2.2. Design of experiments with Response Surface Methodology

Design of experiments (DoE) is a statistical strategy for methodically organizing, carrying out, and analyzing experiments with the objective to optimize and enhance procedures, goods, or systems. It entails carefully modifying a system's input variables (factors) to evaluate their impacts on the desired output response (outcome). DoE is extensively utilized in many industries, including engineering, production, chemistry, and social sciences, to study and comprehend the link between factors and responses in an efficient and effective manner. Response Surface Methodology (RSM) is a subset of DoE that focuses on developing mathematical models to characterize the link between the input factors and the response, it could be used to optimize the experimental results [58,59]. It attempts to identify the ideal settings for the components that will deliver the best potential response. Whenever the connection between variables and response is intricate and non-linear, RSM is very beneficial [60]. RSM represents the answer as a function of the components using polynomial regression models. A second-order polynomial regression model with two components (x_1 and x_2) has the following general form [61,62]:

$$Y = \beta_0 + \beta_1 x_1 + \beta_2 x_2 + \beta_{11} x_1^2 + \beta_{22} x_2^2 + \beta_{12} x_1 x_2 + \varepsilon \tag{1}$$

Wherein, the anticipated response of the variable (output) is denoted by Y. The regression coefficients that were determined based on the data are β_0, β_1, β_2, β_{11}, β_{12}, and β_{22}. x_1 and x_2 are the levels (values) of the two elements under consideration. ε is the error term that represents the amount of residual variation that the model does not explain. RSM's purpose is to calculate the coefficients (β_0, β_1, β_2, β_{11}, β_{12}, and β_{22}) from experimental data and subsequently, employ the model to improve the response by determining which factor values maximize or minimize it. RSM commonly utilizes several experimental designs, like Central Composite Design (CCD) or
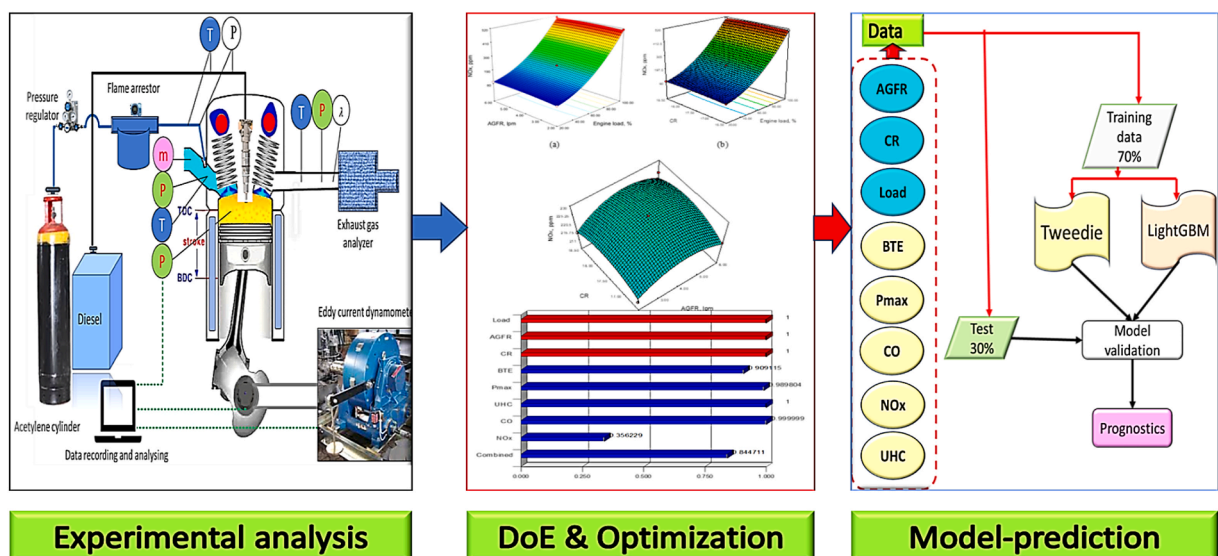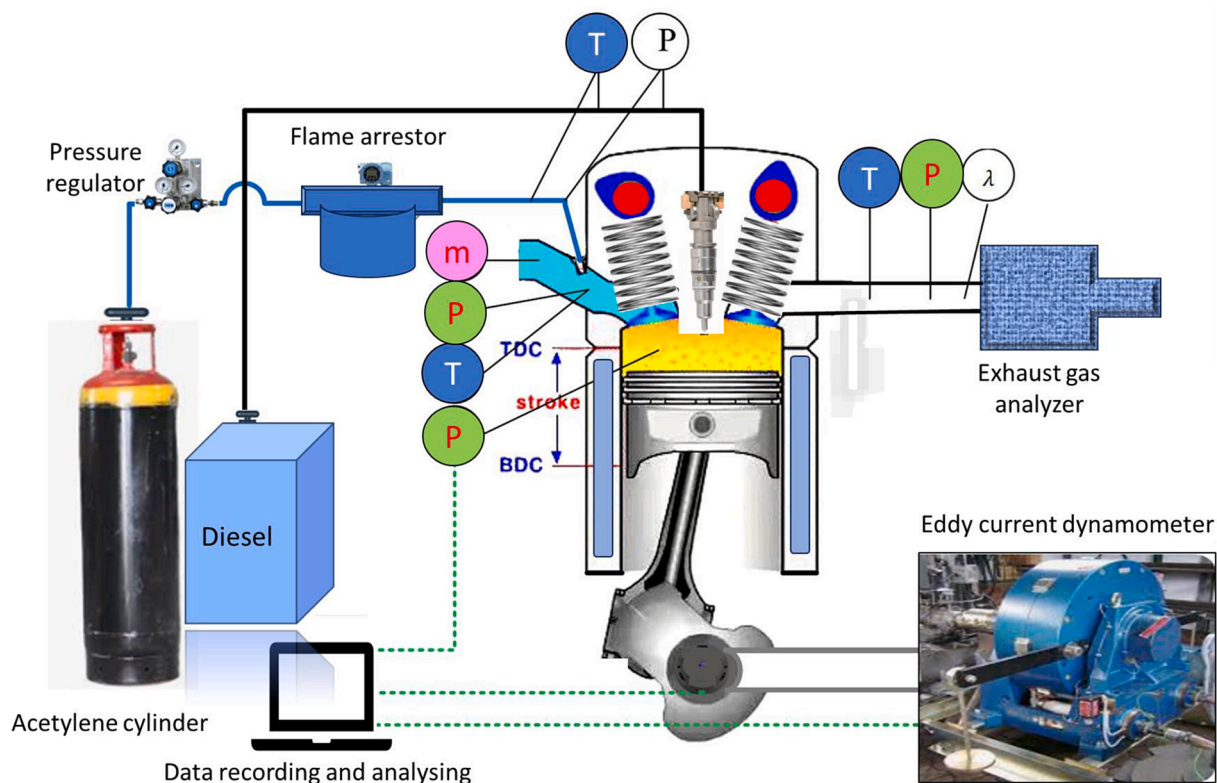

Fig. 1. Schematic diagram of the research.

Fig. 2. Employed engine test setup.

Table 1
Main characteristics of test fuel.

Properties	Diesel	Acetylene
Chemical formulae	$C_{12}H_{26}$	C_2H_2
Density (@ 1.01325 bar and 293 K)	857 kg/m^3	1.092 kg/m^3
Lower calorific value (kJ/kg)	42600	48300
Stoichiometric air-fuel ratio (kg/kg)	14.5	13.2
Cetane number	48	–
Viscosity	2.88 cSt	–

Box-Behnken Design, to do this. These designs allow for efficient investigation of the factor space whilst reducing the number of tests necessary [62].

These designs have been selected for their orthogonality as well as rotatability qualities, which aid in predicting the coefficients with high precision and facilitate simple viewing of the response surface. RSM's mathematical methodology includes regression analysis for calculating coefficients and statistical tests to determine the relevance of components. The model is then utilized to discover ideal factor values (to maximize or decrease the response) by accounting for crucial points such as stationary points and employing numerical optimization methods. Overall, RSM is a strong and effective approach that integrates experimental design, statistical evaluation, and mathematical modeling to improve processes and systems, reducing time and resources while meeting performance goals.

2.3. Uncertainty analysis

For the uncertainty analysis associated with any experimental investigation, the broadly established Perturbation techniques are applied [63]. Fig. 3 shows the relative errors and uncertainty associated with various performance metrics. In the case of peak pressure measurement, the relative error (RE) was only 0.05 %, and RE was 1.2 % for engine speed. In the case of engine load RE was 0.2 % while it was 1 % for the lower calorific value (LCV) of the fuel. In the case of emission measurement, it was altogether 2.65 %. These disparities underline the need for precise measurement and calibration methodologies in engine performance evaluation. On the other hand, The AGFR uncertainty was estimated as 1.1 %, it was 1.2 % for air flow rate. Uncertainty was 1.6 % and 1.3 % for BTE and brake power respectively.
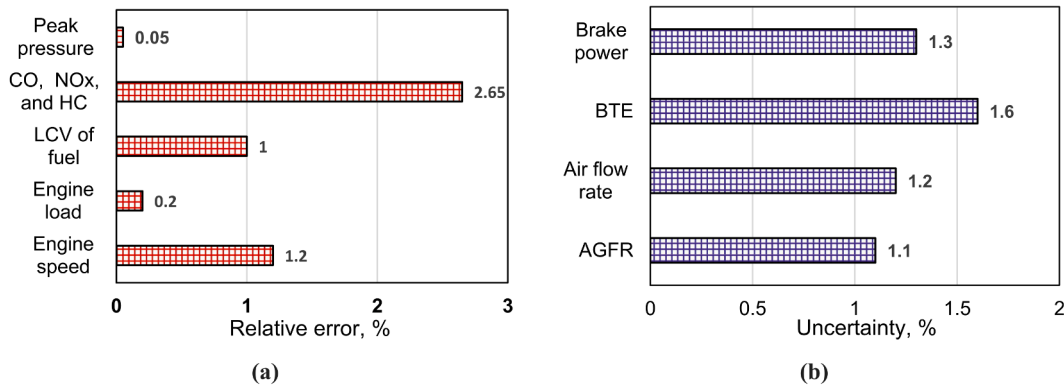
Fig. 3. (a) Relative error **(b)** Uncertainty.

2.4. Design matrix

The RSM-based Design of Experiment (DoE) was used to formulate an experiment strategy for conducting the experiments as shown in Table 2. The Box-Behnken design was used in the present study. Box-Behnken Design, an intriguing variation of RSM, offers a novel way to experimental design. This strategy enables researchers to investigate three variables at the same time, making it perfect for optimizing answers with minimal resources. Box-Behnken Design quickly estimates primary impacts, quadratic effects, and two-way relationships by integrating fewer runs while keeping the design's orthogonality [64]. Its rotatability enables researchers to investigate response surfaces from various angles, aiding the identification of optimal factor values. Box-Behnken Design is a tempting choice for an array of research and manufacturing processes, where it reveals hidden insights and accelerates breakthroughs in numerous sectors, thanks to its ability to reduce experimental error and deliver exact model predictions.

2.5. Analysis of variance

Analysis of variation (ANOVA) is a method of statistics that evaluates the variation across groups to help uncover the secrets hidden inside data. ANOVA has evolved as a basic tool in many domains such as psychology, biology, engineering, and economics [58,65,66]. The core of ANOVA is its capacity for comparing means and examining the influence of various factors on data variance. ANOVA allows researchers to identify whether or not differences between groups are significant by splitting total variability into separate sources [67]. The ANOVA outcomes for BTE and Pmax are listed in Table 3, while for emission data is listed in Table 4.

2.6. Prognostics analysis with modern machine learning

2.6.1. Tweedie

Incorporating the statistical characteristics of the Tweedie distribution, the Tweedie machine learning approach adds a unique dimension to predictive modelling [68]. When represented mathematically:

Table 2
Design matrix for experiment.

Run	Control factors			Response variables				
	Load, %	AGFR, lpm	CR	BTE, %	Pmax, bar	UHC, ppm	CO, ppm	NOx, ppm
3	60	2	18.5	21.8	69.8	71	111	215
9	100	2	17.5	27.4	74.9	71	112	511
12	20	2	17.5	11.5	46	100	137	86
15	60	2	16.5	21.1	68.4	72	145	211
1	100	4	18.5	28.7	76.9	64	102	506
2	20	4	18.5	11.3	46.5	92	108	96
4	60	4	17.5	23.4	71.3	59	112	229
6	60	4	17.5	23.4	71.3	59	112	229
7	60	4	17.5	23.4	71.3	59	112	229
10	20	4	16.5	11.3	46	96	128	94
11	60	4	17.5	23.4	71.3	59	112	229
13	60	4	17.5	23.4	71.3	59	112	229
17	100	4	16.5	27	76	66	124	507
5	60	6	18.5	22.5	69.4	64	106	224
8	60	6	16.5	21.7	68.7	67	124	218
14	20	6	17.5	11.1	45.4	93	119	94
16	100	6	17.5	28.4	75.4	64	120	506

Table 3
ANOVA outcomes for engine performance.

Source	BTE			Pmax		
	SS	Value of 'F'	p' value (Prob > F)	SS	Value of 'F'	p' value (Prob > F)
Model	598.72	6898.87	<0.0001	2169.89	4927.56	<0.0001
Model	549.46	56981.17	<0.0001	1779.06	36360.38	<0.0001
P-Load	0.45	46.80	0.0002	0.01	0.10	0.7585
Q-AGFR	1.28	132.74	<0.0001	1.53	31.30	0.0008
R–CR	0.49	50.81	0.0002	0.30	6.18	0.0418
PQ	0.72	74.93	<0.0001	0.04	0.82	0.396
PR	0.00	0.26	0.6263	0.12	2.50	0.1576
QR	37.89	3929.82	<0.0001	364.17	7442.86	<0.0001
P^2	2.69	279.45	<0.0001	10.44	213.47	<0.0001
Q^2	2.87	297.19	<0.0001	1.78	36.36	0.0005
Residual	0.07			0.34		
Lack of Fit	0.07			0.34		
Pure Error	0.00			0.00		
Cor Total	598.79			2170.23		

Table 4
ANOVA outcomes for emission data.

Source	UHC			CO			NOx		
	SS	Value of 'F'	p' value (Prob > F)	SS	Value of 'F'	p' value (Prob > F)	SS	Value of 'F'	p' value (Prob > F)
Model	3295.24	2562.96	<0.0001	1957.118	22.06	0.0002	369558	5155.77	<0.0001
P-Load	1682.00	11774.00	<0.0001	144.50	14.66	0.006	344450	43249.33	<0.0001
Q-AGFR	84.50	591.50	<0.0001	162.00	16.43	0.0048	45.13	5.67	0.0489
R–CR	12.50	87.50	<0.0001	1104.50	112.05	<0.0001	15.13	1.90	0.2106
PQ	0.00	0.00	1	169.00	17.14	0.004	42.25	5.30	0.0547
PR	1.00	7.00	0.0331	1.00	0.10	0.759	2.25	0.28	0.6115
QR	1.00	7.00	0.0331	64.00	6.49	0.038	1.00	0.13	0.7335
P^2	1216.84	8517.89	<0.0001	16.84	1.71	0.232	24964.2	3134.52	<0.0001
Q^2	151.58	1061.05	<0.0001	269.47	27.34	0.001	191.84	24.09	0.0017
R^2	51.58	361.05	<0.0001	9.47	0.96	0.359	116.05	14.57	0.0066
Residual	1.00			69			55.75		
Lack of Fit	1.00			69			55.75		
Pure Error	0.00			0			0		
Cor Total	3296.24			2026.118			369614		

$$y_i = \mu_i + \Phi y_i^{(p-1)} - \gamma y_i^{(q-1)} + \epsilon_i \tag{2}$$

In Eq. (2), the y_i denotes response variable, μ_i shows mean value, Φ shows the dispersion parameter, and γ also denotes the dispersion parameter. This formulation incorporates the interaction that exists between the response's mean and variance in addition to an extensive range of data kinds, such as continuous, number, and sparse data. The Tweedie ML technique can handle complicated datasets and provide reliable predictions because of its versatile mathematical underpinnings, particularly in situations when conventional models fall short. This ground-breaking approach opens new doors for enhanced prediction capabilities and useful insights across a variety of disciplines by seamlessly incorporating statistical insights into ML frameworks [69,70]. Due to its flexibility in handling multiple data types and complex variance frameworks, the Tweedie ML method, which has its roots in its original mathematical formulation, finds use in many different fields. Similar to how it helps in modelling over-dispersed species abundance data in ecology. It is appropriate for examining consumer records of transactions or social media interactions since its incorporation into predictive analytics enhances the precision of forecasts in settings characterized by diverse data sources [71,72].

The Tweedie machine learning strategy does, however, have some drawbacks, just like any other technique. When the fundamental information considerably departs from these assumptions, it may produce inferior results due to its reliance on the Tweedie distribution assumptions. In addition, rigorous calibration is needed to establish the optimum values for the dispersion parameters (and), which could prove difficult in practice. Despite these drawbacks, the method's distinctive integration of distribution features into ML opens the door for more precise and nuanced modelling across a variety of domains, bridging the gap between statistical insights and based data predictions.

2.6.2. LighGBM

The LightGBM ML approach offers a solid mathematical basis for predictive modeling and is renowned for its effective gradient-boosting architecture. At its core, LightGBM minimizes loss while iteratively incorporating weak learners to optimize an objective function. The weighted forecasts of all weak learners are added up to create the final prediction, with the weights being based on how

much each weak learner contributed to reducing the loss [73]. In the case for a regression objective having N training samples consisting of M features. Here the loss function is defined as following if y_i and $\hat{y}_i$, are target value and predicted value, respectively.

$$Loss\ function = \left(y_i, \widehat{y}_i\right) \tag{3}$$

In case of each iteration 't', the loss function's negative gradient comparative to previous model's predictions is estimated as:

$$g_i^{(t)} = -\frac{\partial L\left(y_i, \widehat{y}_i^{t-1}\right)}{\partial \widehat{y}_i^{t-1}} \tag{4}$$

The construction of tree in case of LightGBM grows in leafwise manner. At each node 'm' of the tree the optimized split is such a way to minimize the loss function. In this case if 'S' represents sample set reaching leaf node 'm'. The optimized point of split is found by:

$$split_m = \arg\ min_{split} \sum_{i \in S} L\left(y_i, \widehat{y}_i^{(t-1)} + split\right) \tag{5}$$

On the tree construction completion, the output value in respect of each leaf node m is estimated using a weighted sum of negative gradient of the sample in the leaf:

$$leaf\_output_m = -\frac{\sum_{i \in S} g_i^{(t)}}{\sum_{i \in S} h_i^{(t)} + \lambda} \tag{6}$$

This presents a simplified overview of the LightGBM process which employs iteratively fitting trees to the negative gradients of the loss function and updating the model's predictions consequently.

The leaf-wise tree growth approach of the method adds more mathematical sophistication. In order to generate more informative splits, it chooses the leaf with the highest delta loss to expand. By adding regularisation terms in its objective function, the LightGBM method also addresses overfitting by balancing the trade-off between bias and variance. With its histogram-based methodology, continuous characteristics are quantized into discrete bins, which enables quick computations and graceful handling of missing values [73,74]. Due to its high computational efficiency, LightGBM is well-suited for real-time or huge dataset applications. Its depth-first growth method, though, might make it more sensitive to outliers. Additionally, parameter adjustment, which includes learning rate and number of leaves, calls for careful thought. However, LightGBM's role as a high-performance tool for diverse ML tasks, from classification to regression, and from ranking to recommendation algorithms, is supported by its use of mathematical elegance and optimization approaches [75,76].

3. Results and discussion

3.1. Correlation among data

The data values gathered through extensive lab-based testing were checked for correlation to reveal statistical linkage among data columns. It was observed that a high correlation (0.96) exists between engine load and BTE, and 0.97 between engine load and NOx emission. This shows that at higher engine loads higher BTE and NOx are observed. On the other side, the acetylene gas flow rate shows a slightly positive effect on BTE while it shows negative effects on UHC and CO emission. This is attributed to the fact that in a constant-speed engine, the fuel supply is controlled with a mechanical governor fitted on the engine. At higher loads, to maintain the engine speed constant, a higher amount of fuel is supplied to the combustion chamber [77,78]. This results in higher temperature and pressure in the combustion chamber resulting in improved BTE and higher generation NOx [79–81]. Similarly, CR shows positive effects on BTE peak pressure and NOx. The low values of correlation are caused by quadratic terms since the effects of AGFR and CR are not linear. The correlation plot is depicted in Fig. 4.

3.2. Brake thermal efficiency

The F-value of the analysis, with a value of 6898.87, suggests that the predictive value is very significant. The possibility of seeing a "Model F-value" of this size owing to noise is a mere 0.01 %. This implies that the model is not an outcome of random chance, but rather a meaningful representation of the data's inherent relationships. Furthermore, the values of "Prob > F″ for different model terms are investigated in order to establish their importance. When "Prob > F″ is less than 0.0500, it indicates that the model terms are statistically noteworthy. The words A, B, C, AB, AC, A^2, B^2, and C^2 are all relevant model terms in this scenario. Values larger than 0.1000, on the contrary, imply that the predictive terms are not significant. If there are multiple inconsequential model terms, except those essential for sustaining hierarchy, reducing them may be advantageous to enhance model performance. The computed standard deviation is 0.098, while the R-squared value is 0.9999, suggesting that the model accounts for a significant amount of the overall variation in the data. Furthermore, the Adjusted R-squared score of 0.9997 validates this conclusion and suggests that the model fits the data well. The Coefficient of Variation (C.V.%) is 0.46, indicating that the relative volatility of the model is fairly low. The Predicted R-squared value of 0.9982 agrees with the Adjusted R-squared number of 0.9997, confirming that the model's predictive capability is adequate. The BTE model can be expressed as:
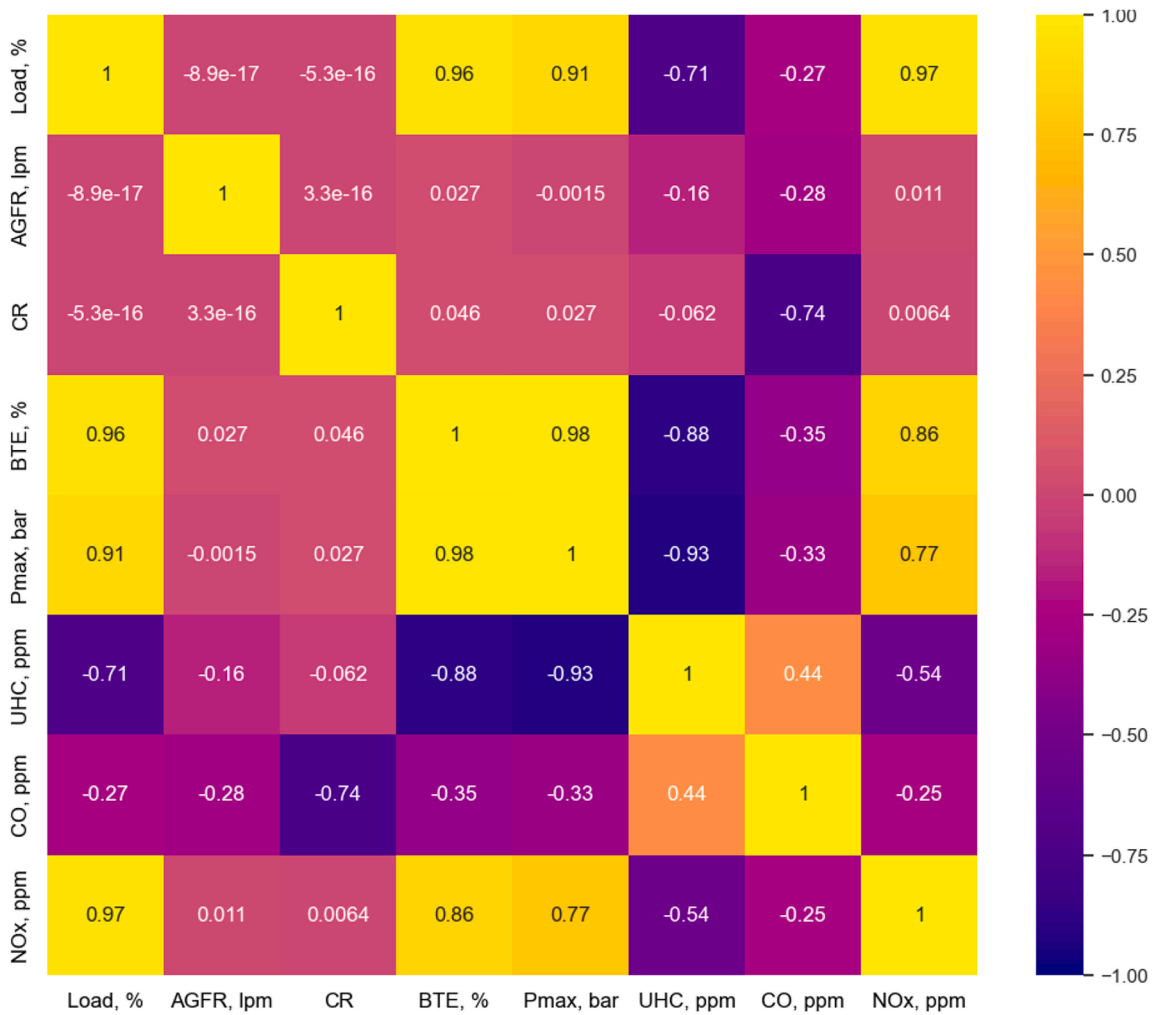
Fig. 4. Correlation plot.

$$BTE = -246.03 + 0.23\,P + 1.24\,Q + 28.59\,R + 0.0044\,PQ$$
$$+ 0.011\,PR + 0.0125\,QR - 0.0018\,\hat{P}2 - 0.2\,\hat{Q}2 - 0.825\hat{R}2 \tag{2}$$

Herein, P denotes the acetylene gas flow rate, Q represents engine load, and Q denotes the compression ratio of the test engine.

Adequacy Precision, which evaluates the signal-to-noise ratio, is an important metric for determining model dependability. A ratio above four is regarded as ideal, and the Adequacy Precision in this example is 232.193, suggesting a high signal-to-noise ratio. The finding adds to the model's usefulness for exploring the design space. In summary, statistical analysis of parameters shows that the model is very significant and valid for the supplied data. The model has strong predictive power and dependability, making it a helpful tool for exploring the design space and making educated decisions based on the variables' correlations. The surface diagram for BTE is depicted in Fig. 5.

As engine load increases, so does the power demand, culminating in increasing fuel consumption along with higher combustion temperatures. The engine performs closer to its intended capacity under raised loads, resulting in better thermal efficiency, as shown in Fig. 5a and b. Excessive loads, on the contrary, can increase mechanical losses and decrease thermal efficiency owing to friction and other inefficiencies [82,83]. In a diesel engine, using acetylene gas as an alternative fuel can change the combustion parameters. Acetylene gas has a greater flame speed along with energy content than diesel, allowing for faster and more efficient burning [84]. When the acetylene flow rate is modified, it can result in greater fuel-air mixing and more thorough combustion, which improves the thermal efficiency of the brakes [85], as depicted in Fig. 5c. Throughout the compression stroke, a larger compression ratio generates increased air temperature and pressure. This, in turn, improves combustion efficiency by compressing and heating the air-fuel combination, allowing for greater energy delivery throughout the power stroke and increased BTE [86–88].
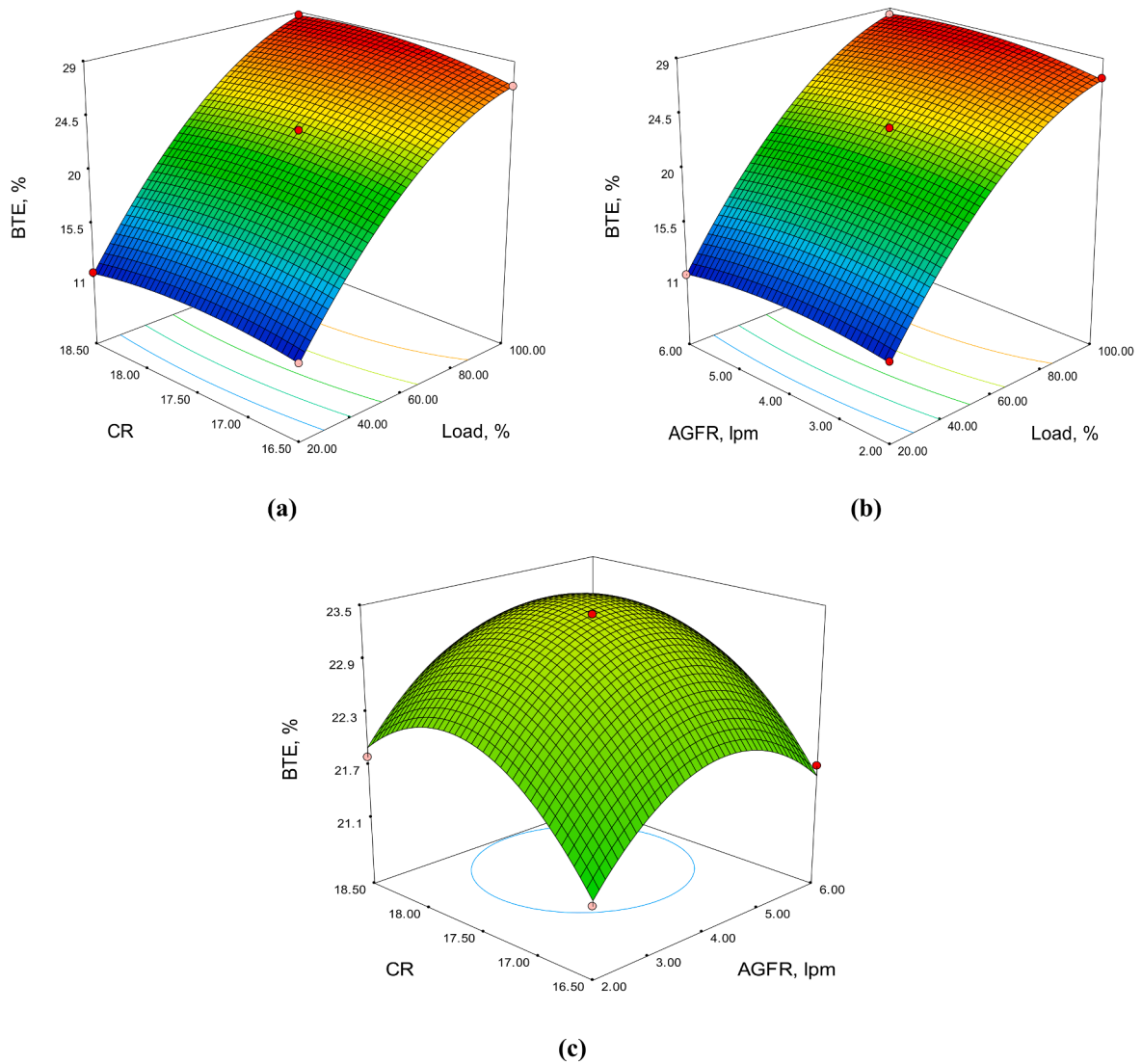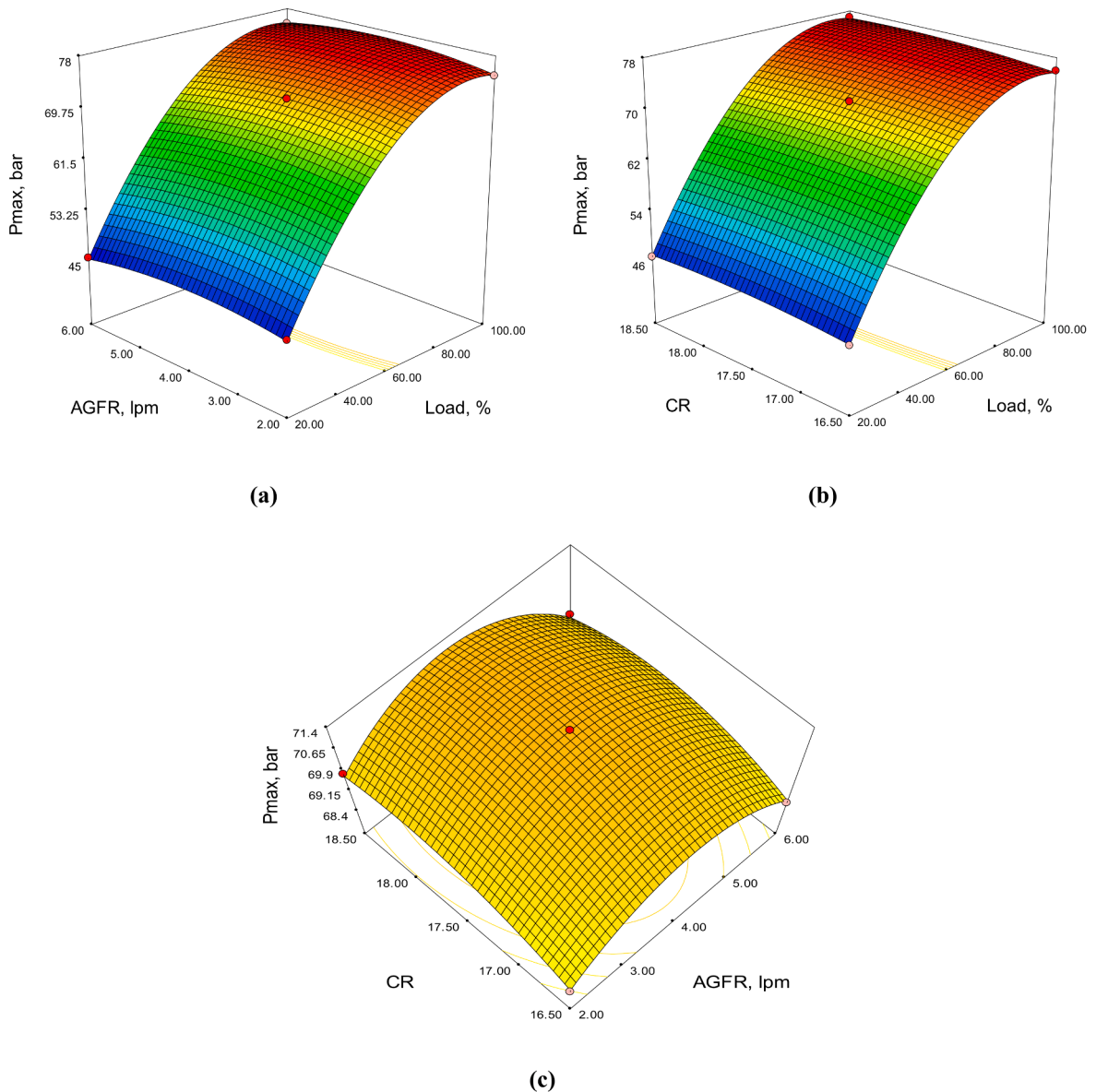
Fig. 5. Surface diagrams for BTE depicting the effects of **(a)** CR and engine load; **(b)** Acetylene gas flow rate and engine load; **(c)** CR and Acetylene gas flow rate.

3.3. Peak cylinder pressure

The model for Pmax developed using ANOVA is given in Eq. (3). The exceptional "Model F-value" of 4927.56 emphasizes the model's relevance, meaning that such an as big "Model F-Value" is extremely unlikely to arise due to random noise. This implies that the model incorporates significant correlations between the variables. A closer look at the "Prob > F″ values indicates that numerous model variables, including A, C, AB, A^2, B^2, and C^2, are considered important since their respective probability are less than 0.0500. These key model elements are critical in explaining the variances found in the data, confirming their relevance in the overall model.

$$Pmax = -187.64 + 1.01\,P + 4.46\,Q + 23.39\,R + 0.0034\,PQ + 0.0025\,PR \\ -\ 0.088\,QR - 0.0058\,\widehat{P}2 - 0.394\,\widehat{Q}2 - 0.65\,\widehat{R}2$$

(3)

Model terms with a probability larger than 0.1000, on the other hand, are deemed insignificant. The Forecast R-squared value of 0.9982 corresponds in magnitude with the Adjusted R-squared number of 0.9997, confirming that the model's ability to predict is adequate. Adequacy Precision, which evaluates the signal-to-noise ratio, is an important metric used to assess model dependability. A ratio greater than 4 is regarded as ideal, and the Adequacy Precision in this example is 232.193, demonstrating a high signal-to-noise ratio. The finding adds to the model's usefulness for exploring the design space. In summary, statistical parameter analysis shows that the model is very significant and valid for the supplied data. The model has strong predictive power and dependability, making it a helpful tool for investigating the design space and making educated decisions based on the variables' correlations.

More fuel is introduced into the cylinder as the engine load rises to match the increasing demand for power. As a consequence, more fuel-air mixture is compressed in the cylinder throughout the compression stroke [89]. As a result, compressing an increased amount of mixture leads to higher peak pressures throughout the combustion process, as shown in Fig. 6a. Because acetylene gas is extremely reactive, it accelerates and completes the combustion process of the fuel-air combination [90,91]. When the flow rate of acetylene gas is raised, it introduces more energy into the combustion process, enabling the combustion to proceed more quickly and furiously. As a result, the rate of pressure rise throughout combustion accelerates, resulting in larger cylinder peak pressures, as shown in Fig. 6b. A greater pressure at the final stage of the compression stroke results from a more efficient compression process. Higher compression ratio results in higher cylinder pressures (Fig. 6c), including the peak pressure following combustion [92,93].

3.4. Unburnt hydrocarbon emission

The model possesses an F-value of 2562.96, demonstrating that it is extremely significant. The likelihood of such a significant "Model F-Value" being influenced by noise is under 0.01 %, showing a strong link between the variables. Model terms are of statistical significance if "Prob > F" is less than 0.0500. Model terms A, B, C, AC, BC, A^2, B^2, and C^2 are all important in this scenario, indicating that they have a substantial impact on the model's output. Values larger than 0.1000 for "Prob > F" indicate that the relevant
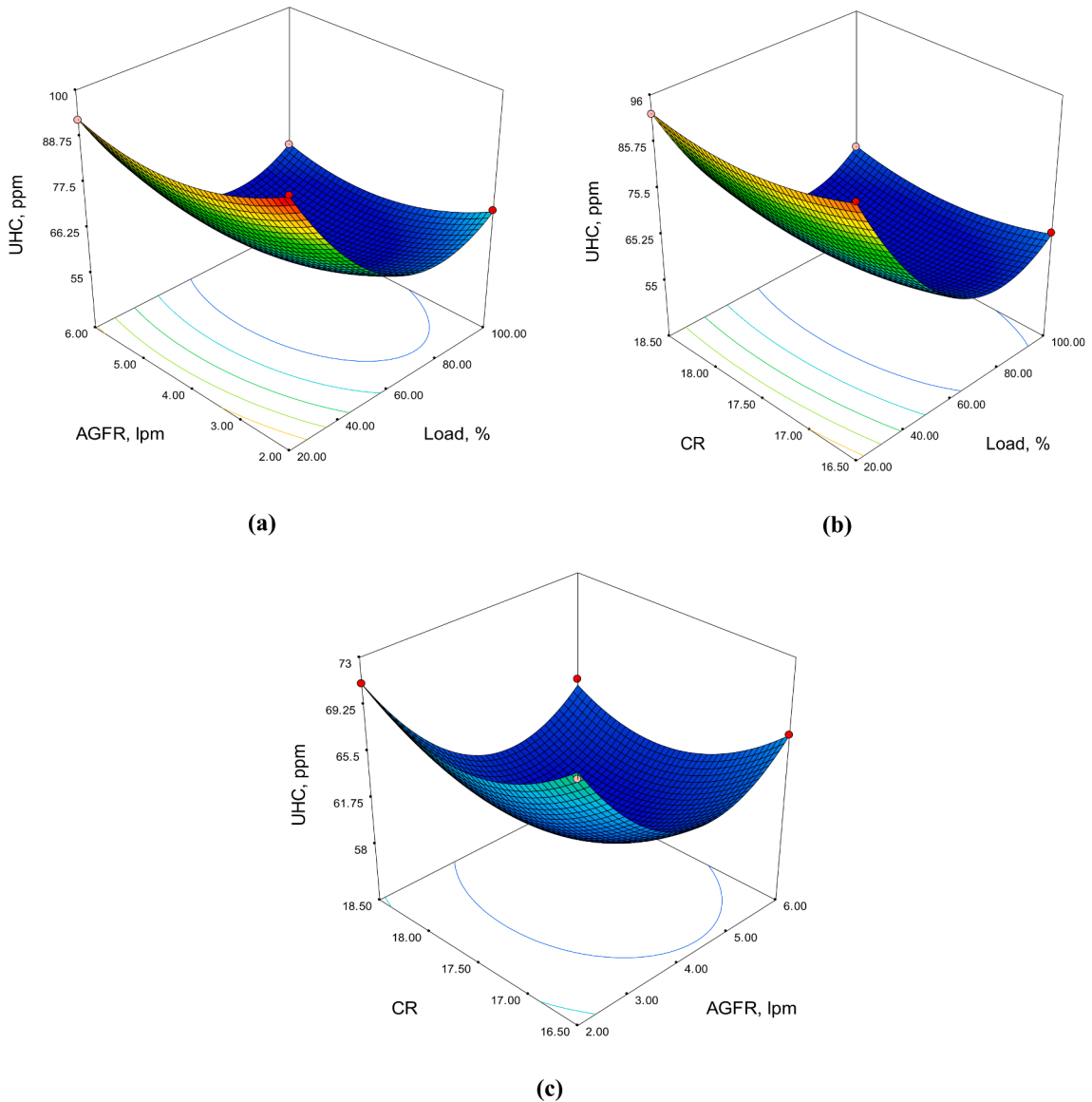
(a)

(b)

(c)

Fig. 6. Surface diagrams for Pmax depicting the effects of **(a)** CR and engine load; **(b)** Acetylene gas flow rate and engine load; **(c)** CR and Acetylene gas flow rate.

model terms are not significant. Reducing model complexity may result in benefits if there are multiple inconsequential model terms (excluding those necessary for hierarchy). The UHC model can be expressed as Eq. (4):

$$UHC = 1238.88 \ - \ 1.86 \, P \ - \ 9.25 \, Q \ - \ 123.5 \, R + 0.0125 \, PR \ - \ 0.25 \, QR + 0.01 \hat{P}2 + 1.5 \, \hat{Q}2 + 3.5 \, \hat{R}2 \tag{4}$$

The model performs well, having an R-squared value of 0.9997 suggesting that it explains nearly all of the variation in the data. This beneficial degree of goodness of fit is reinforced by the Adjusted R-squared of 0.9993. The coefficient of variation is 0.53, indicating that the data is not variable. The "Pred $R^{2''}$" score of 0.9951 corresponds well with the "Adj R^2," demonstrating the model's dependability.

Engine load, AGFR, and CR are all three essential elements that influence the total amount of UHC emissions released by a diesel engine. The larger loads often result in greater-intensity combustion processes. At higher loads, the engine's cylinders endure higher temperatures and pressures, resulting in more complete fuel combustion and, as a result, lower UHC emissions [94]. Indeed, it could be seen the relationship between UHC emissions with compression ratio and engine loads in Fig. 7a. When employed as an additive, acetylene gas improves combustion efficiency by accelerating the ignition and burning of any leftover fuel particles which could be contributing to unburned hydrocarbons, as shown in Fig. 7b [95,96]. It works by encouraging more complete combustion of diesel fuel. Finally, compression flow, as indicated by the compression ratio, is critical. A greater CR causes higher compression tempera-

(a)

(b)

(c)

Fig. 7. Surface diagrams for UHC emission depicting the effects of **(a)** CR and engine load; **(b)** Acetylene gas flow rate and engine load; **(c)** CR and Acetylene gas flow rate.

tures and pressures, therefore improving combustion efficiency, and reducing unburned hydrocarbon production, as shown in Fig. 7c. Finding a satisfying medium between these variables is critical for optimizing engine performance, fuel consumption, and environmental effects, resulting in cleaner and more ecological diesel engine running [97,98].

3.5. Carbon mono-oxide emission

The Model F-value of 22.06 demonstrates that the model is very significant, and it has a 0.02 % chance of attaining such a huge F-value as a result of noise. Model terms have significance when "Prob > F" is less than 0.0500. The words A, B, C, AB, BC, and B^2 are all pertinent in this scenario. Values larger than 0.1000, on the other hand, indicate that the model terms are not significant. Reduce the model if it contains multiple inconsequential model terms. The standard deviation of 3.14, in addition to an R-squared value of 0.9659, indicates that the model describes a significant amount of variability in the data. This inference is supported by the adjusted R-squared value of 0.9222, which indicates a satisfactory fit for the model. The term "Adeq Precision" refers to the signal-to-noise ratio. A ratio larger than 4 is preferred, and the ratio of 17.754 shows a suitably strong signal in this circumstance. As a consequence, this model may be employed to reliably investigate the design space. The model developed for CO emission for the present study can be expressed as:

$$CO = 975.25 - 0.36\,P - 58.13\,Q - 71.5\,R + 0.08\,PQ - 0.0125\,PR + 2\,QR + 0.00125\,\widehat{P}2 + 2\,\widehat{Q}2 + 1.5\,\widehat{R}2 \tag{5}$$

In a CI engine, raising the load may result in more CO emissions. Whenever the engine is running at greater loads, it takes more fuel to create the necessary power, resulting in higher diesel fuel combustion [99,100]. This increased combustion might result in incomplete combustion, which produces more CO as a byproduct. When acetylene gas is put into the engine in regulated proportions, it can improve combustion and minimize CO emissions, as depicted in Fig. 8a and b. The inclusion of acetylene gas in the air-fuel combination can increase combustion efficiency, resulting in more complete burning of diesel fuel and, as a result, fewer CO emissions [101,102]. Higher compression ratios result in higher compression stroke temperatures and pressures, resulting in better combustion, as depicted in Fig. 8c. There is a reduced amount of unburned fuel with enhanced combustion, which equals lower CO emissions. A lower compression ratio, on the contrary, may result in incomplete combustion and increased CO emissions.

3.6. Oxides of nitrogen

The model's relevance and efficacy are revealed via analysis. The model's F value of 5155.77 suggests that the model is very substantial, with only a 0.01 % probability of such a huge F-value being caused by noise. In addition, values less than 0.0500 for "Prob > F" suggest that model elements A, B, A^2, B^2, and C^2 are statistically significant. Values larger than 0.1000, on the other hand, imply that some model terms are not relevant. The model's ability to explain variance in the data has been shown by the standard deviation of 2.82 and R-squared value of 0.9998. Furthermore, the mean of 259.59 and Adjusted R-squared value of 0.9997 reflect the model's great goodness of fit. The mathematical model for NOx emission is expressed as:

$$\begin{aligned} NOx = {} & -1584.56 - 0.097\,P + 12.75\,Q + 185.25\,R - 0.04\,PQ \\ & - 0.019\,PR + 0.25\,QR + 0.048\,\widehat{P}2 - 1.69\,\widehat{Q}2 - 5.25\,\widehat{R}2 \end{aligned} \tag{6}$$

The model's forecasts are in high agreement with the actual data, as demonstrated by the Coefficient of Variation (C.V.) of 1.09 % and the Forecast R-squared value of 0.9976. The model's accuracy in forecasting is measured by the "PRESS" value of 892.00, and the Adequate Precision score of 195.315 shows an adequate signal-to-noise ratio. Finally, the research encourages the model's importance and its ability to predict events with high precision. The "Pred R^{2}" of 0.9976 corresponds precisely with the "Adj R^{2}" of 0.9997, adding to the model's dependability. With a reasonable signal-to-noise ratio, this model can be used with confidence to navigate the design space.

To match the greater torque needs, additional fuel is pumped into the combustion chamber as the engine load increases. During the combustion process, this results in increased pressures and temperatures. Because of the oxidation of nitrogen in the air at elevated temperatures, the generation of NOx increases substantially [103,104]. As a result, larger engine loads tend to generate higher NOx emissions due to the increase in temperature in the combustion process [105,106]. Indeed, it could be seen the relationship between NOx emissions with compression ratio and engine loads as using acetylene in from Fig. 9a. When acetylene enters the engine, it combines with the nitrogen oxides, changing them to nitrogen and carbon dioxide, which are not as hazardous to the environment. As a result, increasing the flow rate of acetylene gas can reduce NOx emissions, as shown in Fig. 9b. Higher CR contributes to higher compression stroke temperatures along with pressures, resulting in improved combustion [107]. Normally, due to the greater combustion temperatures, it may also increase the generation of NOx in the combustion chamber [108]. A lower CR, on the other hand, may result in reduced NOx emissions but may affect engine efficiency and power production, as shown in Fig. 9c.

3.7. Desirability-based optimization

Desirability-based optimization is an effective approach for optimizing numerous responses in a process or mechanism at the same time [109,110]. Researchers may use desirability-based optimization to simultaneously enhance BTE, Pmax, CO, UHC, and NOx emissions in the context of the diesel engine's efficiency and emissions. In desirability-based optimization, the first step is to determine the goal values or ranges for each answer. For example, we would wish to optimize BTE and peak pressure whilst reducing CO, HC, and NOx emissions. Each response will be assigned a desirability function that measures how near it is to the goal value. Then, based on the proximity to the goal, we assign distinct desirability scores to each response. A score of one suggests the reaction reaches or ex-
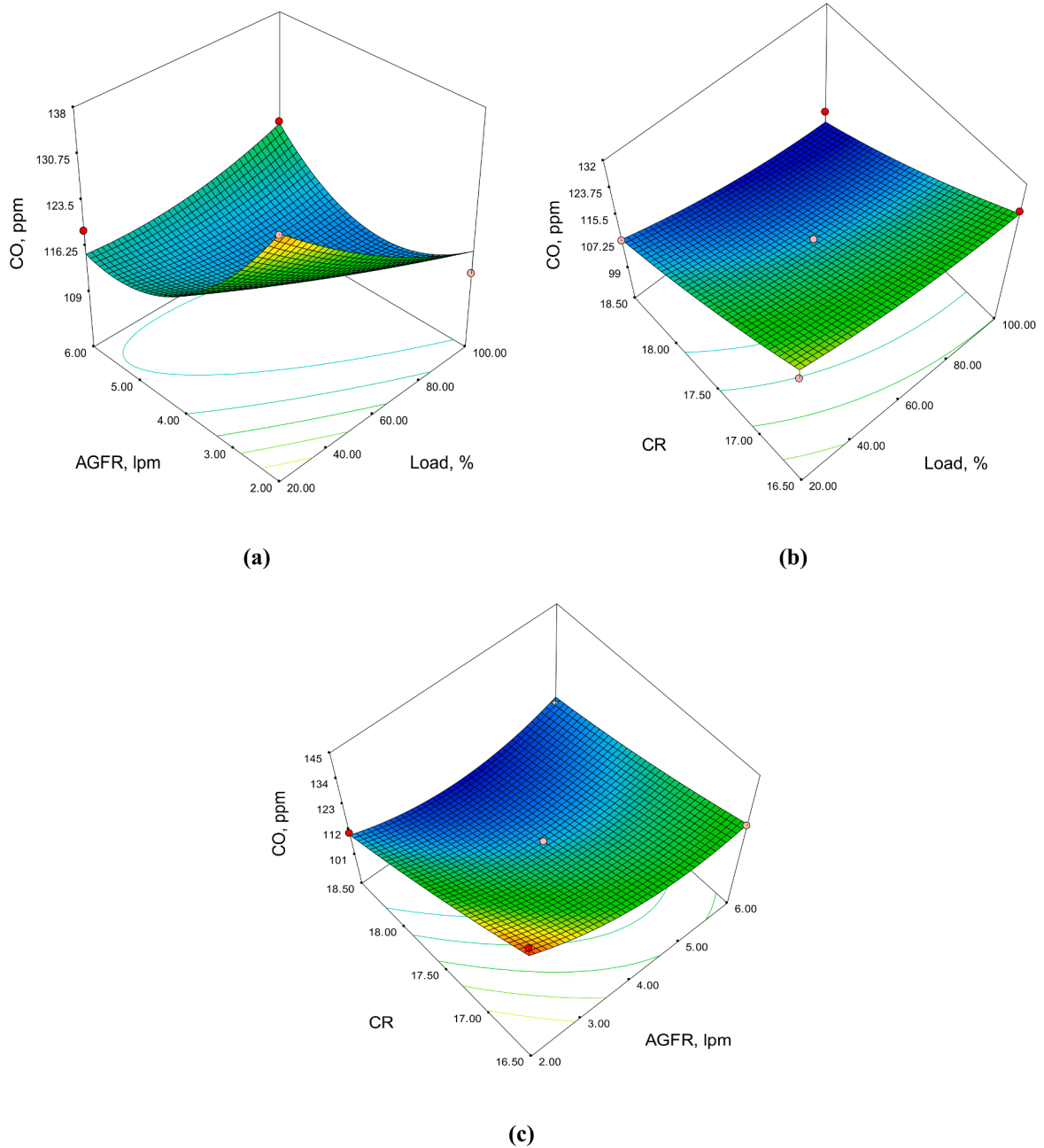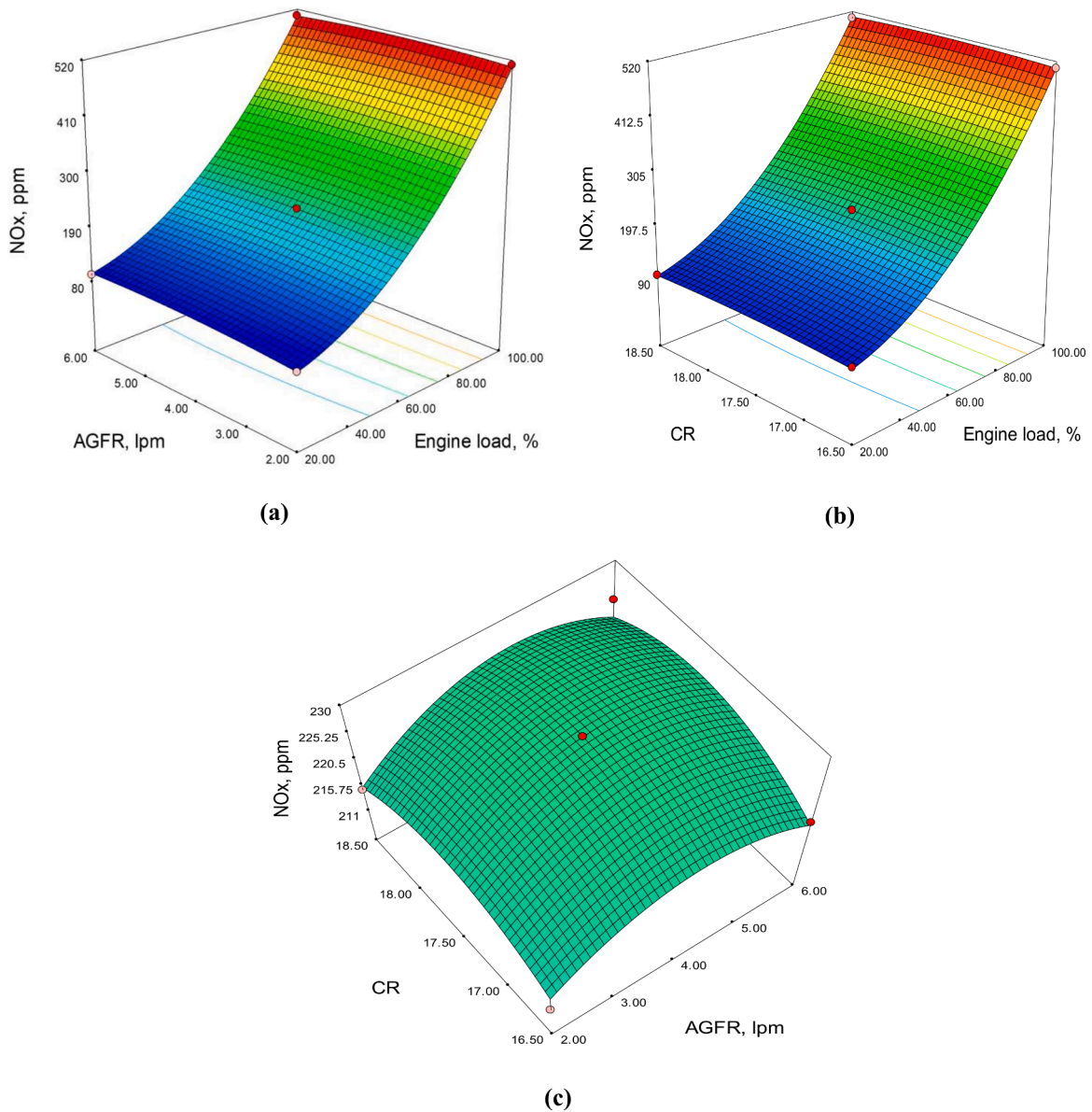
Fig. 8. Surface diagrams for CO emission depicting the effects of **(a)** CR and engine load; **(b)** Acetylene gas flow rate and engine load; **(c)** CR and Acetylene gas flow rate.

ceeds the intended value, whereas a value of zero indicates that it is far from it. Intervals between 0 and 1 denote partial attractiveness. The geometric mean of individual desirability for all responses is used to establish the overall desirability for the engine's efficiency and emissions. The geometric mean method assures that all replies are equally weighted and that no single response dominates the optimization [111,112].

Researchers may use techniques for optimization like the Genetic Algorithm or Particle Swarm Optimization to find the optimal combination of engine operating parameters (engine load, acetylene gas flow rate, and compression ratio). This will provide an ideal set of engine operating settings that maximize BTE and peak pressure while reducing CO, HC, and NOx emissions. Desirability-based optimization offers an in-depth and equitable method for determining the best trade-offs between different options. It enables researchers and engineers to find the optimum acceptable solution for a difficult problem, such as diesel engine performance and emis-

Fig. 9. Surface diagrams for NOx emission depicting the effects of; **(a)** CR and engine load; **(b)** Acetylene gas flow rate and engine load; **(c)** CR and Acetylene gas flow rate.

sions, resulting in environmentally friendly and productive engines in real-world applications. The desirability set in the present study is depicted in Fig. 10.

The optimized operational settings and the outcome at this optimum level is listed in Table 5. Subsequently, the engine was tested at an optimized engine operation setting. The result of engine testing at the optimized setting is also listed in Table 5.

4. Model prediction with machine learning

The data collected with experimental analysis was employed for developing the high-precision ML-based models, for effective forecasting of the engine's output. Both Tweedie and LightGBM ML techniques were used for this purpose. The procedure is depicted in Fig. 11.

It can be observed that both models performed efficiently during forecasting. In the case of the BTE model as depicted in Fig. 12a for the Tweedie-based model and Fig. 13a for LightGBM. The R^2 value for Tweedie based model was almost 1 while it was 0.86 for the based model during model training. However, when the model was tested on fresh data, the R^2 value became 0.99 and 0.8 for the Tweedie and LightGBM-based models, respectively. The prognostic errors in the models as measured with MSE were 0 and 6.09 for
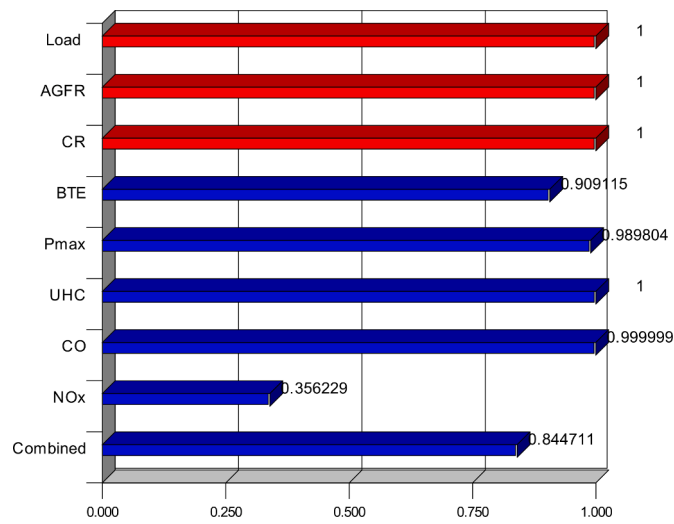
Fig. 10. Desirability levels.

Table 5
RSM optimized results, validation, and error.

Operating parameter	Optimized level	Response variable	Result at optimized setting	Experimental values	% Error
AGFR, lpm	4.48	BTE, %	27.1	26.5	2.21
Engine load, %	81.25	Pmax, bar	76.58	73	4.67
CR	18	UHC, ppm	56.2	60	6.76
		CO, ppm	104	110	5.76
		NOx, ppm	360	372	3.33
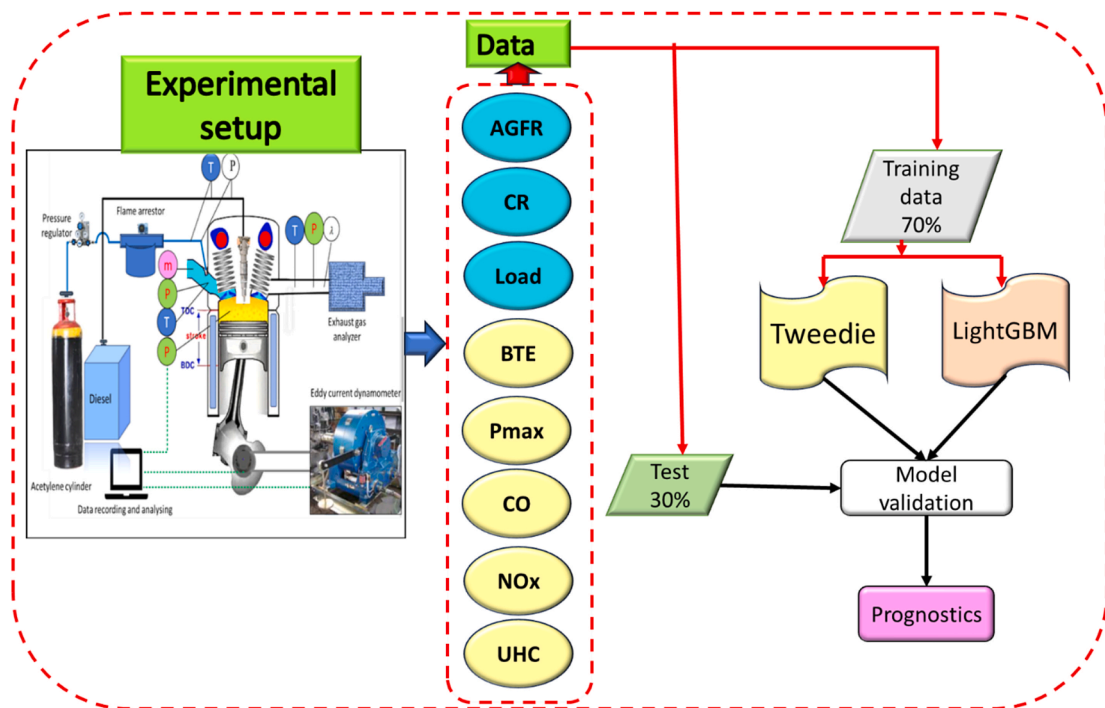
Fig. 11. Schematics of model development.
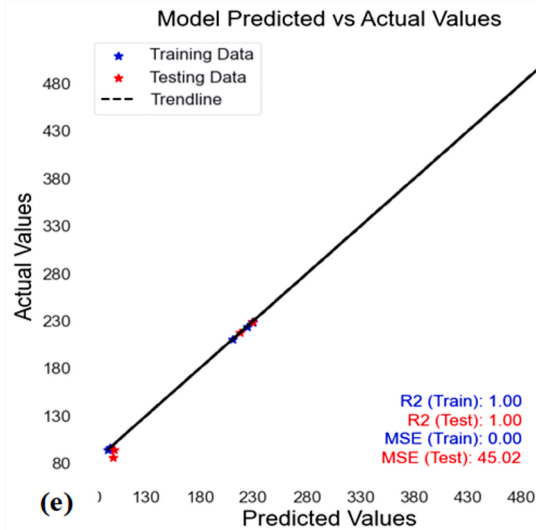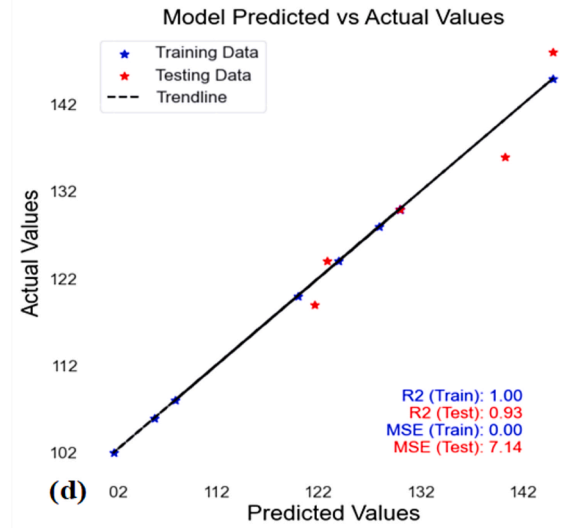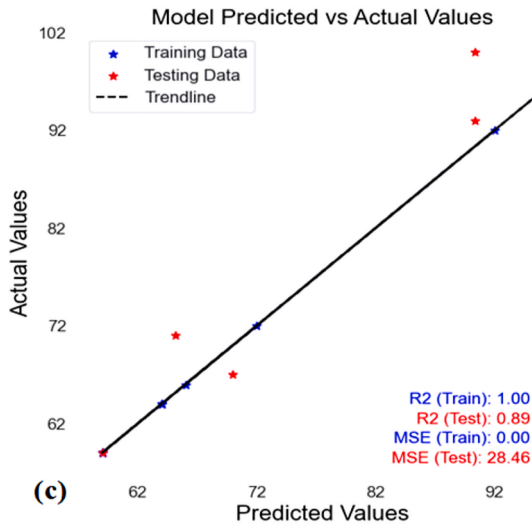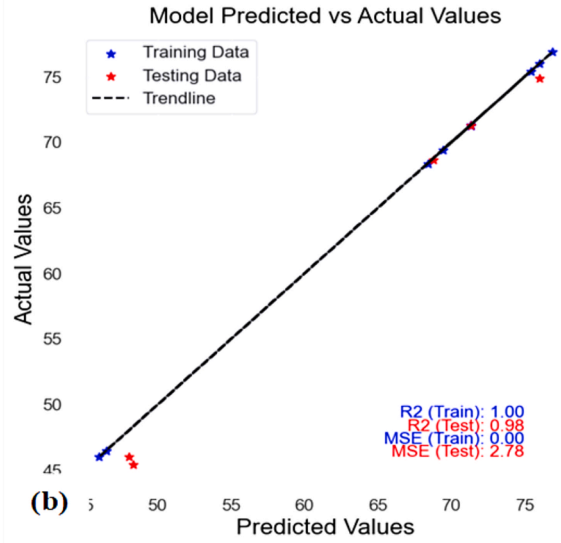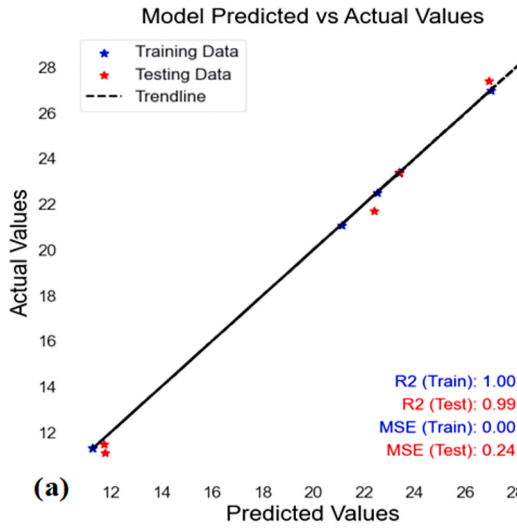
Fig. 12. Actual vs model predicted values using Tweedie ML for (a) BTE; (b) Pmax; (c) UHC emission; (d) CO emission; (e) NOx emission.

Tweedie and LightGBM-based models during the training of models. The MSE values became 0.24 and 8.5 during the model test for Tweedie and LightGBM-based models. The low model errors and high coefficient of determinates shows a robust model. However, the Tweedie model performed superior to the LightGBM model. In the case of the Pmax model, as shown in Fig. 12b for the Tweedie-based model and Fig. 13b for the LightGBM. During model training, the R^2 value for the Tweedie-based model was nearly one, whereas it was 0.74 for the LightGBM-based model. However, when the model was evaluated on new data, the R^2 values for the Tweedie and LightGBM-based models were 0.98 and 0.67, respectively. During model training, the prognostic errors in the models as determined by MSE were 0 and 28.62 for the Tweedie and LightGBM-based models, respectively. During model testing, the MSE values for Tweedie and LightGBM-based models were 2.78 and 54.37, respectively. A robust model is shown by low model errors and a high coefficient of determinates. However, the Tweedie model outperformed the LightGBM model, in this case too.

In the case of a UHC emission model, as shown in Fig. 12c for a Tweedie-based model and Fig. 13c for a LightGBM-based model. During model training, the R^2 value for the Tweedie-based model was nearly one, whereas the R^2 value for the LightGBM-based model was poor at 0.53. However, when the model is evaluated on new data, the R^2 value increases to 0.89 and 0.38 for the Tweedie and LightGBM-based models, respectively. During model training, the prognostic errors in the models, as measured by MSE, were 0 and 74.55 for the Tweedie and LightGBM-based models, respectively. During model testing, the MSE values for Tweedie and Light-GBM-based models reached 28.46 and 153.89, respectively. The low model errors and high coefficient of determinates indicates a strong model. The Tweedie model, on the other hand, outperformed the LightGBM model.

As shown in Fig. 12d for a Tweedie-based model and Fig. 13d for a LightGBM-based model, for the CO emission model. During model training, the R^2 number for the Tweedie-based model was almost 1, but it was only 0.9 for the LightGBM-based model. But when the model is tested on new data, the R^2 number goes up to 0.93 for the Tweedie-based model and 0.65 for the LightGBM-based model. During model training, the Tweedie-based models had a mean squared error (MSE) of 0 and the LightGBM-based models had a mean squared error of 5.01. During model testing, the MSE values for Tweedie-based models reached 7.14 and those for LightGBM-based models hit 10.81. The high coefficient of determinates and low model mistakes show that the model is strong. The LightGBM model, on the other hand, wasn't as good as the Tweedie model. For a NOx emission model, this is shown in Fig. 12e for a Tweedie-based model and in Fig. 13e for a LightGBM-based model. During model training, the R^2 number was almost 1, for both models. It was the same during the test also. During model training, the mean squared error (MSE) for the Tweedie-based models was 0 and it was 31.14 for the LightGBM-based models. During tests, the MSE values for models based on Tweedie reached 45.02, and those for models based on LightGBM reached 52.16. The model is strong because it has a high coefficient of determinates and low model errors. On the other hand, the LightGBM model wasn't as good as the Tweedie model.

5. Conclusions

In this study, acetylene gas was employed as the primary fuel and diesel as the pilot fuel The study effectively fine-tuned the diesel engine's operating parameters by using a desirability-based optimization method. Also, two modern machine learning approaches namely Tweedie and LightGBM were employed to develop prediction models for engine operating parameters. The main outcomes are as follows.

o The optimized parameters estimated were 4.48 lpm for AGFR, 81.25 % for engine load, along with 18 for compression ratio. At the optimized engine setting, the model predicted BTE was 27.1 %, and the peak cylinder pressure was 73 bar. In this case, the UHC emission was 56.2 ppm, CO emission was 104 ppm, and NOx emission was 360 ppm at the optimized engine setting.
o At the optimized engine setting, all the model-predicted results were observed well within the 2.21–6.76 % range. The R^2 value for Tweedie-based models was in the range of 0.89–1 while it was in the range of 0.38–1 in the case of the LightGBM-based models.
o On the prediction error fronts, the mean squared error was in the range of 0.24–45.04 in the case of Tweedie-based models and it was 8.5–153.89. Even though both machine learning methods worked well, Tweedie was much better at making predictions than LightGBM-based models, both in terms of R^2 and MSE.

Finally, the optimization of operating parameters in dual-fuel diesel engines employing acetylene gas as the primary fuel offers an achievable approach to improving engine performance and lowering emissions. This study paves the way for future research into improving dual-fuel engines utilizing alternative fuels by employing intelligent approaches.

CRediT authorship contribution statement

Van Giao Nguyen: Writing – review & editing, Methodology, Conceptualization. **Brijesh Dager:** Writing – original draft, Methodology, Investigation. **Ajay Chhillar:** Writing – review & editing, Conceptualization. **Prabhakar Sharma:** Writing – original draft, Validation, Software, Methodology, Investigation, Data curation. **Sameh M. Osman:** Writing – review & editing, Methodology. **Duc Trong Nguyen Le:** Methodology, Investigation, Conceptualization. **Jerzy Kowalski:** Writing – review & editing, Methodology. **Thanh Hai Truong:** Writing – review & editing, Methodology. **Prem Shanker Yadav:** Conceptualization, Writing – review & editing. **Dao Nam Cao:** Methodology, Investigation. **Viet Dung Tran:** Methodology, Conceptualization, Writing – review & editing.
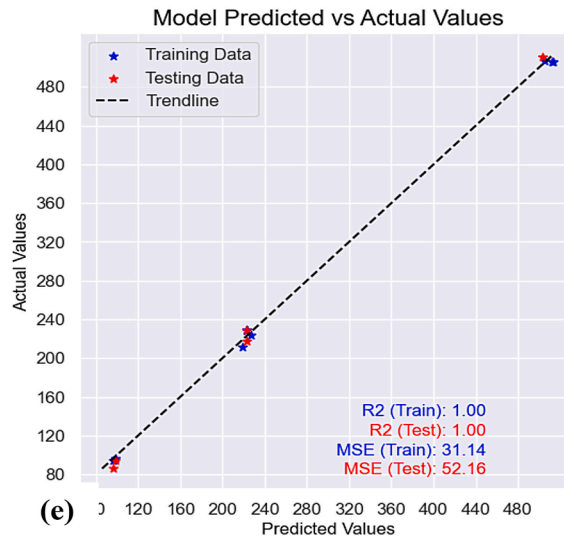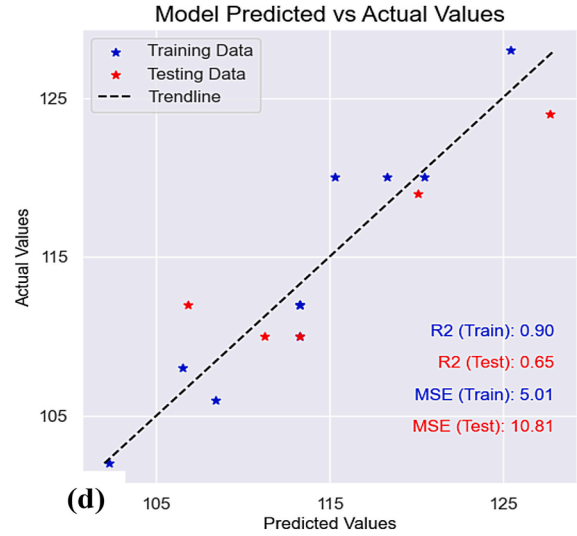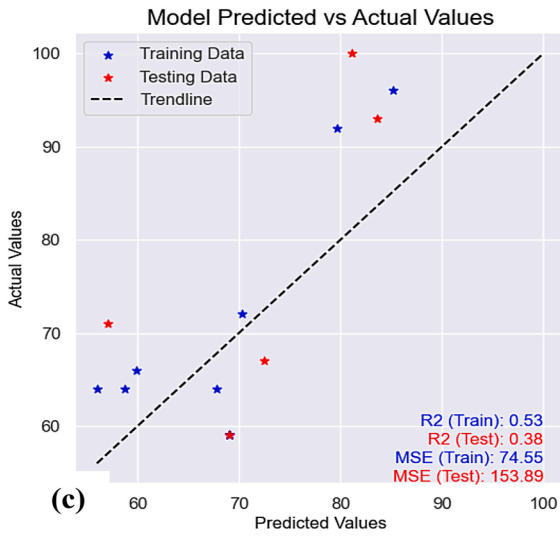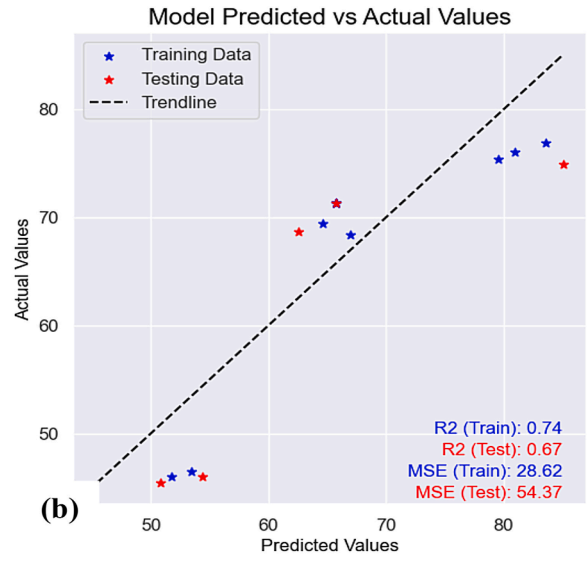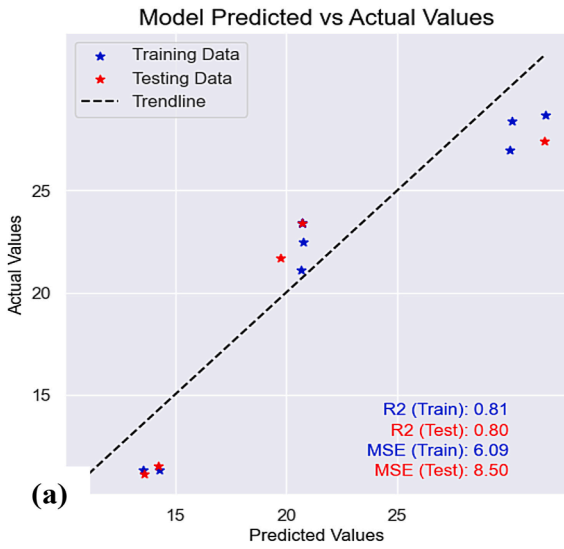
Fig. 13. Actual vs model predicted values using LightGBM for (a) BTE; (b) Pmax; (c) UHC emission; (d) CO emission; (e) NOx emission.

Declaration of competing interest

The authors declare that they have no known competing financial interests or personal relationships that could have appeared to influence the work reported in this paper.

Data availability

Data will be made available on request.

Acknowledgement

References

[1] A. Grubler, C. Wilson, N. Bento, B. Boza-Kiss, V. Krey, D.L. McCollum, et al., A low energy demand scenario for meeting the 1.5 °C target and sustainable development goals without negative emission technologies, Nat. Energy 3 (2018) 515–527, https://doi.org/10.1038/s41560-018-0172-6.

[2] P. Gümplová, Normative View of natural resources—global Redistribution or human rights–based approach? Hum. Right Rev. 22 (2021) 155–172.

[3] N.I. Ilham, M.Z. Hussin, N.Y. Dahlan, E.A. Setiawan, Prospects and challenges of Malaysia's distributed energy resources in business models towards zero–carbon emission and energy security, Int. J. Renew. Energy Dev. 11 (2022) 1089–1100.

[4] M.S. Mu'mina, M. Yaqinb, M.S. Anama, Does energy transition matter to sustainable development in ASEAN? Int. J. Renew. Energy Dev. 13 (2024) 191–205.

[5] H. Bakır, Ü. Ağbulut, A.E. Gürel, G. Yıldız, U. Güvenç, M.E.M. Soudagar, et al., Forecasting of future greenhouse gas emission trajectory for India using energy and economic indexes with various metaheuristic algorithms, J. Clean. Prod. 360 (2022) 131946, https://doi.org/10.1016/j.jclepro.2022.131946.

[6] M.M. Maja, S.F. Ayano, The impact of population growth on natural resources and farmers' capacity to adapt to climate change in low-income countries, Earth Syst Environ 5 (2021) 271–283, https://doi.org/10.1007/s41748-021-00209-6.

[7] A.J. Barid, H. Hadiyanto, Hyperparameter optimization for hourly PM2.5 pollutant prediction, J Emerg Sci Eng 2 (2024) e15, https://doi.org/10.61435/jese.2024.e15.

[8] Z. Chen, W. Wei, L. Song, B.-J. Ni, Hybrid water electrolysis: a new sustainable avenue for energy-saving hydrogen production, Sustain Horizons 1 (2022) 100002, https://doi.org/10.1016/j.horiz.2021.100002.

[9] T.T.H. Nguyen, Y.-T. Tu, G.L. Diep, T.K. Tran, N.H. Tien, F. Chien, Impact of natural resources extraction and energy consumption on the environmental sustainability in ASEAN countries, Resour. Pol. 85 (2023) 103713.

[10] S. Mondal, D. Palit, Challenges in natural resource management for ecological sustainability, in: Nat. Resour. Conserv. Adv. Sustain., Elsevier, 2022, pp. 29–59.

[11] Z. Zahoor, M.I. Latif, I. Khan, F. Hou, Abundance of natural resources and environmental sustainability: the roles of manufacturing value-added, urbanization, and permanent cropland, Environ. Sci. Pollut. Res. 29 (2022) 82365–82378.

[12] X.P. Nguyen, A.T. Hoang, A.I. Ölçer, T.T. Huynh, Record decline in global CO2 emissions prompted by COVID-19 pandemic and its implications on future climate change policies, Energy Sources, Part A Recover Util Environ Eff (2021) 1–4, https://doi.org/10.1080/15567036.2021.1879969.

[13] K.O. Yoro, M.O. Daramola, CO2 emission sources, greenhouse gases, and the global warming effect, in: Adv. Carbon Capture, Elsevier, 2020, pp. 3–28.

[14] T. Yusaf, A.S. Faisal Mahamude, K. Kadirgama, D. Ramasamy, K. Farhana, A. Dhahad H, et al., Sustainable hydrogen energy in aviation – a narrative review, Int. J. Hydrogen Energy (2023), https://doi.org/10.1016/j.ijhydene.2023.02.086.

[15] M.A. Fayad, A.A. Radhi, S.H. Omran, F.M. Mohammed, Influence of environment-friendly fuel additives and fuel injection pressure on soot nanoparticles characteristics and engine performance, and nox emissions in CI diesel engine, J Adv Res Fluid Mech Therm Sci 88 (2021) 58–70, https://doi.org/10.37934/arfmts.88.1.5870.

[16] M.A. Fayad, S.I. Ibrahim, S.H. Omran, F.J. Martos, T. Badawy, A.M. Al Jubori, et al., Experimental effect of CuO2 nanoparticles into the RME and EGR rates on NOX and morphological characteristics of soot nanoparticles, Fuel 331 (2023) 125549, https://doi.org/10.1016/j.fuel.2022.125549.

[17] V.N. Nguyen, K. Rudzki, D. Marek, N.D.K. Pham, M.T. Pham, P.Q.P. Nguyen, et al., Understanding fuel saving and clean fuel strategies towards green maritime, Pol. Marit. Res. 30 (2023) 146–164, https://doi.org/10.2478/pomr-2023-0030.

[18] A.Y. Kian, S.C. Lim, On the potential of solar energy for chemical and metal manufacturing plants in Malaysia, Int. J. Adv. Sci. Eng. Inf. Technol. 13 (2023) 1898–1904, https://doi.org/10.18517/ijaseit.13.5.19052.

[19] Rostin, A.A. Muthalib, R.M. Iswandi, A. Putera, L.O.M. Harafah, N.H. Aswad, et al., Achievement of performance and evaluation of green city development indicators for sustainable cities (SDGs) in 2030, Int. J. Adv. Sci. Eng. Inf. Technol. 13 (2023) 1393–1403, https://doi.org/10.18517/ijaseit.13.4.18243.

[20] W. Zeńczak, A.K. Gromadzińska, Preliminary analysis of the use of solid biofuels in a ship's power system, Pol. Marit. Res. 27 (2020) 67–79, https://doi.org/10.2478/pomr-2020-0067.

[21] L. Changxiong, Y. Hu, Z. Yang, H. Guo, Experimental study of fuel combustion and emission characteristics of marine diesel engines using advanced fuels, Pol. Marit. Res. 30 (2023) 48–58, https://doi.org/10.2478/pomr-2023-0038.

[22] A.T. Hoang, A. Pandey, Z. Huang, R. Luque, K.H. Ng, A.M. Papadopoulos, et al., Catalyst-based synthesis of 2,5-dimethylfuran from carbohydrates as a sustainable biofuel production route, ACS Sustain. Chem. Eng. 10 (2022) 3079–3115, https://doi.org/10.1021/acssuschemeng.1c06363.

[23] K.D. Choudhary, A. Nayyar, M.S. Dasgupta, Effect of compression ratio on combustion and emission characteristics of C.I. Engine operated with acetylene in conjunction with diesel fuel, Fuel 214 (2018) 489–496, https://doi.org/10.1016/j.fuel.2017.11.051.

[24] A.T. Hoang, S. Nižetić, H.C. Ong, W. Tarelko, T.H. Le, M.Q. Chau, et al., A review on application of artificial neural network (ANN) for performance and emission characteristics of diesel engine fueled with biodiesel-based fuels, Sustain. Energy Technol. Assessments 47 (2021) 101416, https://doi.org/10.1016/j.seta.2021.101416.

[25] V.H. Dong, P. Sharma, Optimized conversion of waste vegetable oil to biofuel with Meta heuristic methods and design of experiments, J Emerg Sci Eng 1 (2023) 22–28, https://doi.org/10.61435/jese.2023.4.

[26] T.X. Nguyen-Thi, T.M.T. Bui, Effects of injection strategies on mixture formation and combustion in a spark-ignition engine fueled with syngas-biogas-hydrogen, Int. J. Renew. Energy Dev. 12 (2023) 118–128, https://doi.org/10.14710/ijred.2023.49368.

[27] M. Fiore, V. Magi, A. Viggiano, Internal combustion engines powered by syngas: a review, Appl. Energy 276 (2020) 115415, https://doi.org/10.1016/j.apenergy.2020.115415.

[28] H. Yaqoob, Y.H. Teoh, M.A. Jamil, M. Gulzar, Potential of tire pyrolysis oil as an alternate fuel for diesel engines: a review, J. Energy Inst. 96 (2021) 205–221, https://doi.org/10.1016/j.joei.2021.03.002.

[29] I. Veza, A.D. Karaoglan, E. Ileri, S.A. Kaulani, N. Tamaldin, Z.A. Latiff, et al., Grasshopper optimization algorithm for diesel engine fuelled with ethanol-biodiesel-diesel blends, Case Stud. Therm. Eng. 31 (2022) 101817, https://doi.org/10.1016/j.csite.2022.101817.

[30] W. Olszewski, M. Dzida, V.G. Nguyen, D.N. Cao, Reduction of CO 2 emissions from offshore combined cycle diesel engine-steam turbine power plant powered

by alternative fuels, Pol. Marit. Res. 30 (2023) 71–80, https://doi.org/10.2478/pomr-2023-0040.

[31] G. Labeckas, S. Slavinskas, J. Rudnicki, R. Zadrąg, The effect of oxygenated diesel-N-butanol fuel blends on combustion, performance, and exhaust emissions of a turbocharged CRDI diesel engine, Pol. Marit. Res. 25 (2018) 108–120, https://doi.org/10.2478/pomr-2018-0013.

[32] A.T. Hoang, V.V. Pham, 2-Methylfuran (MF) as a potential biofuel: a thorough review on the production pathway from biomass, combustion progress, and application in engines, Renew. Sustain. Energy Rev. 148 (2021) 111265, https://doi.org/10.1016/j.rser.2021.111265.

[33] H. Li, X. Ma, T.U. PoWen, H. Xu, S.-J. Shuai, A. Ghafourian, Numerical study of DMF and gasoline spray and mixture preparation in a GDI engine, SAE Technical Paper 17 (2013) 2013-01-1592.

[34] S. Wang, L. Yao, Effect of engine speeds and dimethyl ether on methyl decanoate HCCI combustion and emission characteristics based on low-speed two-stroke diesel engine, Pol. Marit. Res. 27 (2020) 85–95, https://doi.org/10.2478/pomr-2020-0030.

[35] Q.B. Doan, X.P. Nguyen, V.V. Pham, T.M.H. Dong, M.T. Pham, T.S. Le, Performance and emission characteristics of diesel engine using ether additives: a review, Int. J. Renew. Energy Dev. 11 (2022) 255–274, https://doi.org/10.14710/ijred.2022.42522.

[36] S. Serbin, K. Burunsuz, D. Chen, J. Kowalski, Investigation of the characteristics of a low-emission gas turbine combustion chamber operating on a mixture of natural gas and hydrogen, Pol. Marit. Res. 29 (2022) 64–76, https://doi.org/10.2478/pomr-2022-0018.

[37] A.T. Hoang, A. Pandey, F.J. Martinez De Osés, W.-H. Chen, Z. Said, K.H. Ng, et al., Technological solutions for boosting hydrogen role in decarbonization strategies and net-zero goals of world shipping: challenges and perspectives, Renew. Sustain. Energy Rev. 188 (2023) 113790, https://doi.org/10.1016/j.rser.2023.113790.

[38] Z. Stelmasiak, J. Larisch, J. Pielecha, D. Pietras, Particulate matter emission from dual fuel diesel engine fuelled with natural gas, Pol. Marit. Res. 24 (2017) 96–104, https://doi.org/10.1515/pomr-2017-0055.

[39] R. Zhao, L. Xu, X. Su, S. Feng, C. Li, Q. Tan, et al., A numerical and experimental study of marine hydrogen–natural gas–diesel tri-fuel engines, Pol. Marit. Res. 27 (2020) 80–90, https://doi.org/10.2478/pomr-2020-0068.

[40] G. Singh, S. Sharma, J. Singh, S. Kumar, Y. Singh, M.H. Ahmadi, et al., Optimization of performance, combustion and emission characteristics of acetylene aspirated diesel engine with oxygenated fuels: an Experimental approach, Energy Rep. 7 (2021) 1857–1874, https://doi.org/10.1016/j.egyr.2021.03.022.

[41] P. Jiang, G. Zhao, H. Zhang, T. Ji, L. Mu, X. Lu, et al., Towards carbon neutrality of calcium carbide-based acetylene production with sustainable biomass resources, Green Energy Environ 9 (2024) 1068–1078, https://doi.org/10.1016/j.gee.2022.12.004.

[42] K. Gupta, K. Suthar, S.K. Jain, G Das Agarwal, A. Nayyar, Design and experimental investigations on six-stroke SI engine using acetylene with water injection, Environ. Sci. Pollut. Res. 25 (2018) 23033–23044, https://doi.org/10.1007/s11356-018-2407-2.

[43] S. Muthuswamy, M. Veerasigamani, Impact of secondary fuel injector in various distance on direct injection diesel engine using acetylene-bio diesel in reactivity controlled compression ignition mode, Energy Sources, Part A Recover Util Environ Eff (2020) 1–15, https://doi.org/10.1080/15567036.2020.1810177.

[44] G.M. Lionus Leo, S. Murugapoopathi, G. Thodda, S.M. Baligidad, R. Jayabal, M. Nedunchezhiyan, et al., Optimisation and environmental analysis of waste cashew nut shell oil biodiesel/cerium oxide nanoparticles blends and acetylene fumigation in agricultural diesel engine, Sustain. Energy Technol. Assessments 58 (2023) 103375, https://doi.org/10.1016/j.seta.2023.103375.

[45] R. Raman, N. Kumar, Comparative assessment of di-ethyl ether/diesel blends on the performance, and emission characteristics in acetylene dual fuel engine, Int. J. Engine Res. 24 (2023) 2692–2707, https://doi.org/10.1177/14680874221132325.

[46] S. Rajaram Koli, Y.V. Hanumantha Rao, Study of low compression ratio on the performance of diesel engine in dual fuel operation with different flow rates of acetylene, Fuel 284 (2021) 118969, https://doi.org/10.1016/j.fuel.2020.118969.

[47] E. Rokni, A. Moghaddas, O. Askari, H. Metghalchi, Measurement of laminar burning speeds and investigation of flame stability of acetylene (C2H2)/air mixtures, J. Energy Resour. Technol. 137 (2015).

[48] S. Sharma, D. Sharma, S.L. Soni, D. Singh, A. Jhalani, Performance, combustion and emission analysis of internal combustion engines fuelled with acetylene – a review, Int. J. Ambient Energy 43 (2022) 622–640, https://doi.org/10.1080/01430750.2019.1663369.

[49] M. Sonachalam, P. PaulPandian, V. Manieniyan, Emission reduction in diesel engine with acetylene gas and biodiesel using inlet manifold injection, Clean Technol. Environ. Policy 22 (2020) 2177–2191, https://doi.org/10.1007/s10098-020-01968-y.

[50] S. Sharma, D. Sharma, S.L. Soni, D. Singh, A. Jhalani, Performance, combustion and emission analysis of internal combustion engines fuelled with acetylene – a review, Int. J. Ambient Energy 43 (2022) 622–640, https://doi.org/10.1080/01430750.2019.1663369.

[51] S. Tangöz, M. Ilhak, S. Akansu, N. Kahraman, Experimental investigation of performance and emisSIons of an SI engine fueled BY BY acetylene-methane and acetylene-hydrogen blends, Fresenius Environ. Bull. 27 (2018) 4174–4185.

[52] D.L. Hilden, R.F. Stebar, Evaluation of acetylene as a spark ignition engine fuel, Int. J. Energy Res. 3 (1979) 59–71, https://doi.org/10.1002/er.4440030107.

[53] M.İ. İlhak, R. Doğan, S.O. Akansu, N. Kahraman, Experimental study on an SI engine fueled by gasoline, ethanol and acetylene at partial loads, Fuel 261 (2020) 116148, https://doi.org/10.1016/j.fuel.2019.116148.

[54] K.D. Choudhary, A. Nayyar, M.S. Dasgupta, Effect of compression ratio on combustion and emission characteristics of C.I. Engine operated with acetylene in conjunction with diesel fuel, Fuel 214 (2018) 489–496, https://doi.org/10.1016/j.fuel.2017.11.051.

[55] S. Sharma, D. Sharma, S.L. Soni, D. Singh, Experimental investigation on spark-ignition (SI) engine fuelled with acetylene in dual-fuel mode, Int. J. Ambient Energy 43 (2022) 2369–2375, https://doi.org/10.1080/01430750.2020.1735519.

[56] T. Lakshmanan, G. Nagarajan, Experimental investigation on dual fuel operation of acetylene in a DI diesel engine, Fuel Process. Technol. 91 (2010) 496–503, https://doi.org/10.1016/j.fuproc.2009.12.010.

[57] M. Nazarpour, A. Taghizadeh-Alisaraei, A. Asghari, A. Abbaszadeh-Mayvan, A. Tatari, Optimization of biohydrogen production from microalgae by response surface methodology (RSM), Energy 253 (2022) 124059, https://doi.org/10.1016/j.energy.2022.124059.

[58] R.H. Myers, D.C. Montgomery, C.M. Anderson-Cook, Response Surface Methodology: Process and Product Optimization Using Designed Experiments, John Wiley & Sons, 2016.

[59] Nazir N. Desniorita, Sayuti K. Novelina, Sustainable design of biorefinery processes on cocoa pod: optimization of pectin extraction process with variations of pH, temperature, and time, Int. J. Adv. Sci. Eng. Inf. Technol. 9 (2019) 2104–2113, https://doi.org/10.18517/ijaseit.9.6.10670.

[60] E.G. Varuvel, S. Seetharaman, F.J. Joseph Shobana Bai, Y. Devarajan, D. Balasubramanian, Development of artificial neural network and response surface methodology model to optimize the engine parameters of rubber seed oil – hydrogen on PCCI operation, Energy 283 (2023) 129110, https://doi.org/10.1016/j.energy.2023.129110.

[61] L.A. Sarabia, M.C. Ortiz, Response surface methodology, Compr Chemom 1 (2009) 345–390, https://doi.org/10.1016/B978-044452701-1.00083-1.

[62] L.M.S. Pereira, T.M. Milan, D.R. Tapia-Blácido, Using response surface methodology (RSM) to optimize 2G bioethanol production: a review, Biomass Bioenergy 151 (2021) 106166.

[63] R.J. Moffat, Using uncertainty analysis in the planning of an experiment, J Fluids Eng Trans ASME (1985), https://doi.org/10.1115/1.3242452.

[64] P. Sharma, A. Chhillar, Z. Said, S. Memon, Exploring the exhaust emission and efficiency of algal biodiesel powered compression ignition engine: application of box-behnken and desirability based multi-objective response surface methodology, Energies 14 (2021) 5968, https://doi.org/10.3390/en14185968.

[65] M.Q. Chau, V.T. Nguyen, Effects of frequency and mass of eccentric balls on picking force of the coffee fruit for the as-fabricated harvesting machines, Int. J. Adv. Sci. Eng. Inf. Technol. 9 (2019) 1039–1045, https://doi.org/10.18517/ijaseit.9.3.8578.

[66] M.E. Bildirici, CO2 emission, oil consumption and production, economic growth in MENAP countries: ARDL and ANOVA methods, Int. J. Oil Gas Coal Technol. 14 (2017) 264–302.

[67] P. Dimitriou, Z. Peng, D. Lemon, B. Gao, M. Soumelidis, Diesel Engine Combustion Optimization for Bio-Diesel Blends Using Taguchi and ANOVA Statistical Methods, 2013, https://doi.org/10.4271/2013-24-0011.

[68] R.R. Petterle, W.H. Bonat, C.C. Kokonendji, J.C. Seganfredo, A. Moraes, M.G. da Silva, Double Poisson-Tweedie regression models, Int. J. Biostat. 15 (2019), https://doi.org/10.1515/ijb-2018-0119.

[69] W.H. Bonat, C.C. Kokonendji, Flexible Tweedie regression models for continuous data, J. Stat. Comput. Simulat. 87 (2017) 2138–2152, https://doi.org/10.1080/00949655.2017.1318876.

[70] R. Abid, C.C. Kokonendji, A. Masmoudi, Geometric Tweedie regression models for continuous and semicontinuous data with variation phenomenon, AStA Adv Stat Anal 104 (2020) 33–58, https://doi.org/10.1007/s10182-019-00350-8.

[71] C.C. Kokonendji, W.H. Bonat, R. Abid, Tweedie regression models and its geometric sums for (semi-)continuous data, WIREs Comput Stat 13 (2021), https://doi.org/10.1002/wics.1496.

[72] A. Hassine, A. Masmoudi, A. Ghribi, Tweedie regression model: a proposed statistical approach for modelling indoor signal path loss, Int. J. Numer. Model. Electron. Network. Dev. Field. 30 (2017) e2243, https://doi.org/10.1002/jnm.2243.

[73] H. Liu, Q. Xiao, Y. Jin, Y. Mu, J. Meng, T. Zhang, et al., Improved LightGBM-based framework for electric vehicle lithium-ion battery remaining useful life prediction using multi health indicators, Symmetry (Basel) 14 (2022) 1584, https://doi.org/10.3390/sym14081584.

[74] B. Li, G. Chen, Y. Si, X. Zhou, P. Li, P. Li, et al., GNSS/INS integration based on machine learning LightGBM model for vehicle navigation, Appl. Sci. 12 (2022) 5565, https://doi.org/10.3390/app12115565.

[75] Z. Yin, L. Shi, J. Luo, S. Xu, Y. Yuan, X. Tan, et al., Pump feature construction and electrical energy consumption prediction based on feature engineering and LightGBM algorithm, Sustainability 15 (2023) 789, https://doi.org/10.3390/su15010789.

[76] A. Shehadeh, O. Alshboul, R.E. Al Mamlook, O. Hamedat, Machine learning models for predicting the residual value of heavy construction equipment: an evaluation of modified decision tree, LightGBM, and XGBoost regression, Autom. ConStruct. 129 (2021) 103827, https://doi.org/10.1016/j.autcon.2021.103827.

[77] A. Yousefi, M. Birouk, Investigation of natural gas energy fraction and injection timing on the performance and emissions of a dual-fuel engine with pre-combustion chamber under low engine load, Appl. Energy 189 (2017) 492–505, https://doi.org/10.1016/j.apenergy.2016.12.046.

[78] E. Arslan, N. Kahraman, The effects of hydrogen enriched natural gas under different engine loads in a diesel engine, Int. J. Hydrogen Energy 47 (2022) 12410–12420.

[79] S.R. Koli, Y.V.H. Rao, Study of low compression ratio on the performance of diesel engine in dual fuel operation with different flow rates of acetylene, Fuel 284 (2021) 118969.

[80] J. Kowalski, W. Tarelko, NOx emission from a two-stroke ship engine. Part 1: modeling aspect, Appl. Therm. Eng. 29 (2009) 2153–2159, https://doi.org/10.1016/j.applthermaleng.2008.06.032.

[81] S.K. Nayak, S. Nižetić, V.V. Pham, Z. Huang, A.I. Ölçer, V.G. Bui, et al., Influence of injection timing on performance and combustion characteristics of compression ignition engine working on quaternary blends of diesel fuel, mixed biodiesel, and t-butyl peroxide, J. Clean. Prod. 333 (2022) 130160, https://doi.org/10.1016/j.jclepro.2021.130160.

[82] A.V. Prabhu, A. Avinash, K. Brindhadevi, A. Pugazhendhi, Performance and emission evaluation of dual fuel CI engine using preheated biogas-air mixture, Sci. Total Environ. 754 (2021) 142389, https://doi.org/10.1016/J.SCITOTENV.2020.142389.

[83] B.J. Bora, T. Dai Tran, K. Prasad Shadangi, P. Sharma, Z. Said, P. Kalita, et al., Improving combustion and emission characteristics of a biogas/biodiesel-powered dual-fuel diesel engine through trade-off analysis of operation parameters using response surface methodology, Sustain. Energy Technol. Assessments 53 (2022) 102455, https://doi.org/10.1016/j.seta.2022.102455.

[84] P. Deb, A. Paul, Effect of acetylene as a low reactivity fuel on performance, combustion, exergy and emissions of an acetylene/diesel RCCI engine with variable premix ratios, Sustain. Energy Fuels 7 (2023) 4547–4566.

[85] K.R. Lawrence, P. Anchupogu, M. Reddy Reddygari, V. Reddy Gangula, D. Balasubramanian, S. Veerasamy, Optimization of biodiesel yield and performance investigations on diesel engine powered with hydrogen and acetylene gas injected with enriched Jojoba biodiesel blend, Int. J. Hydrogen Energy 50 (2024) 502–523, https://doi.org/10.1016/j.ijhydene.2023.09.166.

[86] L. Zhou, F. Luo, An experimental investigation on the cylinder pressure of a biogas-diesel dual fuel engine, in: Proc. 2016 Int. Conf. Civil, Transp. Environ, Atlantis Press, Paris, France, 2016, https://doi.org/10.2991/iccte-16.2016.146.

[87] N. Khayum, S. Anbarasu, S. Murugan, Combined effect of fuel injecting timing and nozzle opening pressure of a biogas-biodiesel fuelled diesel engine, Fuel 262 (2020) 116505, https://doi.org/10.1016/j.fuel.2019.116505.

[88] P. Rosha, S. Kumar, P. Senthil Kumar, C.N. Kowthaman, S. Kumar Mohapatra, A. Dhir, Impact of compression ratio on combustion behavior of hydrogen enriched biogas-diesel operated CI engine, Fuel 310 (2022) 122321, https://doi.org/10.1016/j.fuel.2021.122321.

[89] A.O. Emiroğlu, M. Şen, Combustion, performance and emission characteristics of various alcohol blends in a single cylinder diesel engine, Fuel 212 (2018) 34–40, https://doi.org/10.1016/j.fuel.2017.10.016.

[90] S.P. Jena, S.K. Acharya, C. Deheri, Thermodynamic analysis of a twin cylinder diesel engine in dual fuel mode with producer gas, Biofuels 7 (2016) 49–55, https://doi.org/10.1080/17597269.2015.1118779.

[91] Ö. Can, E. Öztürk, H.S. Yücesu, Combustion and exhaust emissions of canola biodiesel blends in a single cylinder DI diesel engine, Renew. Energy 109 (2017) 73–82, https://doi.org/10.1016/j.renene.2017.03.017.

[92] V.S. Yaliwal, N.R. Banapurmath, P.G. Tewari, Performance, combustion and emission characteristics of a single-cylinder, four-stroke, direct injection diesel engine operated on a dual-fuel mode using Honge oil methyl ester and producer gas derived from biomass feedstock of different origin, Int. J. Sustain. Eng. 7 (2014) 253–268, https://doi.org/10.1080/19397038.2013.834395.

[93] E.A. Melo-Espinosa, R. Piloto-Rodríguez, Y. Sánchez-Borroto, S. Verhelst, Effect of emulsified fuels based on fatty acid distillates on single cylinder diesel engine performance and exhaust emissions, Appl. Therm. Eng. 120 (2017) 187–195, https://doi.org/10.1016/j.applthermaleng.2017.03.133.

[94] I. Kalargaris, G. Tian, S. Gu, Combustion, performance and emission analysis of a DI diesel engine using plastic pyrolysis oil, Fuel Process. Technol. 157 (2017) 108–115, https://doi.org/10.1016/j.fuproc.2016.11.016.

[95] P. Dubey, R. Gupta, Influences of dual bio-fuel (Jatropha biodiesel and turpentine oil) on single cylinder variable compression ratio diesel engine, Renew. Energy 115 (2018) 1294–1302, https://doi.org/10.1016/j.renene.2017.09.055.

[96] A.K. Agarwal, A. Dhar, D.K. Srivastava, R.K. Maurya, A.P. Singh, Effect of fuel injection pressure on diesel particulate size and number distribution in a CRDI single cylinder research engine, Fuel 107 (2013) 84–89, https://doi.org/10.1016/j.fuel.2013.01.077.

[97] A.K. Agarwal, D.K. Srivastava, A. Dhar, R.K. Maurya, P.C. Shukla, A.P. Singh, Effect of fuel injection timing and pressure on combustion, emissions and performance characteristics of a single cylinder diesel engine, Fuel 111 (2013) 374–383.

[98] M.S. Raihan, E.S. Guerry, U. Dwivedi, K.K. Srinivasan, S.R. Krishnan, Experimental analysis of diesel-ignited methane dual-fuel low-temperature combustion in a single-cylinder diesel engine, J. Energy Eng. 141 (2015), https://doi.org/10.1061/(ASCE)EY.1943-7897.0000235.

[99] M.A. Fayad, A. Tsolakis, F.J. Martos, M. Bogarra, I. Lefort, K.D. Dearn, Investigation the effect of fuel injection strategies on combustion and morphology characteristics of PM in modern diesel engine operated with oxygenate fuel blending, Therm. Sci. Eng. Prog. 35 (2022) 101476, https://doi.org/10.1016/j.tsep.2022.101476.

[100] M.A. Fayad, M.T. Chaichan, H.A. Dhahad, A.A. Al-Amiery, Isahak WNR. Wan, Reducing the effect of high sulfur content in diesel fuel on NOx emissions and PM characteristics using a PPCI mode engine and gasoline–diesel blends, ACS Omega 7 (2022) 37328–37339, https://doi.org/10.1021/acsomega.2c03878.

[101] C. Nayak, S.K. Acharya, R.K. Swain, Emission analysis of different blends of karanja oil with producer gas in a twin-cylinder diesel engine in dual fuel mode, Energy Sources, Part A Recover Util Environ Eff 38 (2016) 821–827.

[102] S.K. Dash, P. Lingfa, S.B. Chavan, Combustion analysis of a single cylinder variable compression ratio small size agricultural DI diesel engine run by Nahar biodiesel and its diesel blends, Energy Sources, Part A Recover Util Environ Eff 42 (2020) 1681–1690, https://doi.org/10.1080/15567036.2019.1604878.

[103] V.G. Bui, T.M.T. Bui, A.T. Hoang, S. Nižetić, T.X. Nguyen Thi, A.V. Vo, Hydrogen-Enriched biogas premixed charge combustion and emissions in direct injection and indirect injection diesel dual fueled engines: a comparative study, J. Energy Resour. Technol. 143 (2021), https://doi.org/10.1115/1.4051574.

[104] A. Suhel, N. Abdul Rahim, M.R. Abdul Rahman, K.A. Bin Ahmad, Engine's behaviour on magnetite nanoparticles as additive and hydrogen addition of chicken fat methyl ester fuelled DICI engine: a dual fuel approach, Int. J. Hydrogen Energy 46 (2021) 14824–14843, https://doi.org/10.1016/j.ijhydene.2021.01.219.

[105] D. Nam, A. Jafrin, T. Johnson, A simulation study on a premixed-charge compression ignition mode-based engine using a blend of biodiesel/diesel fuel under a split injection strategy, Int. J. Adv. Sci. Eng. Inf. Technol. 14 (2024) 451–471, https://doi.org/10.18517/ijaseit.14.2.20007.

[106] T.T. Le, R. Kumar, M.K. Roy, M.K. Mishra, P.K. Mahto, D. Balasubramanian, et al., An experimental assessment of waste transformer oil and palm oil biodiesel blended with diesel fuel on A single cylinder direct in diesel engine, Int. J. Adv. Sci. Eng. Inf. Technol. 14 (2024) 246–258, https://doi.org/10.18517/

ijaseit.14.1.15998.
[107] G. Chen, W. Kong, Y. Xu, Y. Shen, F. Wei, Thermal efficiency and emissions improvement of the lean burn high compression ratio HPDI NG engine at different combustion modes, Appl. Therm. Eng. (2024) 123061.
[108] A.T. Hoang, M. Tabatabaei, M. Aghbashlo, A.P. Carlucci, A.I. Ölçer, A.T. Le, et al., Rice bran oil-based biodiesel as a promising renewable fuel alternative to petrodiesel: a review, Renew. Sustain. Energy Rev. 135 (2021) 110204, https://doi.org/10.1016/j.rser.2020.110204.
[109] E.C. Harrington, The desirability function, Ind Qual Control 21 (1965) 494–498.
[110] X. Lei, J. Shuang, P. Yang, Y. Liu, Parametric study and optimization of dimpled tubes based on Response Surface Methodology and desirability approach, Int. J. Heat Mass Tran. 142 (2019) 118453, https://doi.org/10.1016/j.ijheatmasstransfer.2019.118453.
[111] P. Sharma, D. Balasubramanian, C. Thanh Khai, I. Papla Venugopal, M. Alruqi, J.S.F. Josephin, et al., Enhancing the performance of renewable biogas powered engine employing oxyhydrogen: optimization with desirability and D-optimal design, Fuel 341 (2023) 127575, https://doi.org/10.1016/j.fuel.2023.127575.
[112] P. Sharma, A. Chhillar, Z. Said, S. Memon, Exploring the exhaust emission and efficiency of algal biodiesel powered compression ignition engine: application of box–behnken and desirability based multi-objective response surface methodology, Energies 14 (2021) 1–22, https://doi.org/10.3390/en14185968.